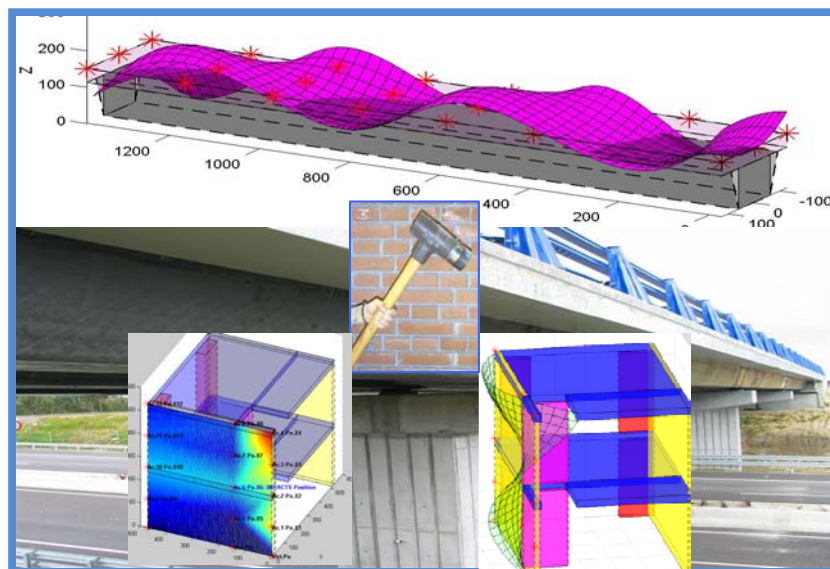




Modal Analysis of Small & Medium Structures by Fast Impact Hammer Testing Method

Daniel Tirelli



EUR 24964 EN - 2011

The mission of the JRC-IPSC is to provide research results and to support EU policy-makers in their effort towards global security and towards protection of European citizens from accidents, deliberate attacks, fraud and illegal actions against EU policies.

European Commission
Joint Research Centre
Institute for the Protection and Security of the Citizen

Contact information

Address: Daniel Tirelli, Joint Research Centre, Via E. Fermi 2749, TP480 21027 Ispra (VA), Italy

E-mail: Daniel.tirelli@jrc.ec.europa.eu

Tel.: +39-0332-785093

Fax: +39-0332-785379

<http://ipsc.jrc.ec.europa.eu/>

<http://www.jrc.ec.europa.eu/>

Legal Notice

Neither the European Commission nor any person acting on behalf of the Commission is responsible for the use which might be made of this publication.

***Europe Direct is a service to help you find answers
to your questions about the European Union***

Freephone number (*):

00 800 6 7 8 9 10 11

(*) Certain mobile telephone operators do not allow access to 00 800 numbers or these calls may be billed.

A great deal of additional information on the European Union is available on the Internet. It can be accessed through the Europa server <http://europa.eu/>

JRC JRC66055

EUR 24964 EN
ISBN 978-92-79-21479-0
ISSN 1831-9424
â[â10.2788/80576

Luxembourg: Publications Office of the European Union

© European Union, 201F

Reproduction is authorised provided the source is acknowledged

Printed in Italy

Acknowledgementu

The research leading to these results has received funding from the European Community's Seventh Framework Program [FP7/2007-2013] under grant agreement n° 227887.

The author expresses his gratitude to Acciona Infraestructuras for supporting the project and providing the beam specimen as part of the PROMETEO project .

My thanks go to Patrick Petit, and Ismael Vadillo Torre, for the technical help in the experimental part and instrumentation and to Georges Magonette and Eugenio Gutierrez for the constant support in developing the method here described.

Contents

1	Introduction.....	1
2	The Fast Impact Hammer Testing (FIHT) Method	1
2.1	The reasons to develop the method.....	1
2.2	The differences between the FIHT method with respect classical Hammer methods.....	2
3	Structure Description and Methodology Employed	2
4	The Fast Impact Hammer Test (FIHT) Method Description and Limitations	3
4.1	Importance of the output transducer position	4
4.2	Remarks on the different steps when using the FIHT	5
5	Signals Processing	5
5.1	General schema.....	5
5.2	Automatic Check of the Measurements by Coherence Histograms	7
5.3	Maps of the FRFs amplitude.....	10
6	Modal Parameters Extraction	12
6.1	Principle of the fast extraction used in the FIHT.....	12
6.2	Criteria for optimal grouping (= solution).....	13
	F1 definition:	13
	F2 definition:	13
	Solution definition:.....	14
6.3	Physical meaning of the functions F1, F2 and of the Solution.....	14
6.4	Representation and results of the parameter extraction.....	16
7	Mode Shapes.....	17
7.1	Mode shape calculation	17
7.2	Mode shapes representation.....	18
7.3	Short Analysis of the method accuracy on mode shapes examples.....	18
8	Implementation of the Logarithmic Decrement in the FIHT Method for Accurate Damping Measurement.....	21
9	Conclusion	23
	References	24
		Annex 1 26

Table of figures

Figure 1: General view of the structure on left and input (Hammer) and output (Accelerometer) transducers used for modal testing	2
Figure 2: Structure design with the output transducers positions (red -black), and the map of the inputs (Impacts).....	3
Figure 3: Example of test description including the channel attribution and transducers coordinates.	3
Figure 4: Analytical results to find the minimum amplitude of the first six bending modes expected along the beam.....	5
Figure 5: Processing time signals and frequency analysis for modal extraction by the Fast Impact Hammer Testing (FIHT)	6
Figure 6: example of the mean FRF of one point position on right, and on left the respective coherence function of the same set of measurements.....	7
Figure 7: Coherence histogram of the FRF on row data, and for one position. One colour by output transducer.	7
Figure 8: From left to right, example of displacement and force time history with relative FRF and coherence.....	8
Figure 9: example of distribution of the coherence values for one test (5 impacts) and for all the transducers.....	8
Figure 10: Example of the map of the filtered coherence for 2 types of transducers: displacement (a), and accelerometer (b).	9
Figure 11: Example of FRFs magnitude of the test no: 1 to 10 (5 impacts each) and acceleration measured in position Z4	10
Figure 12: Example of maps of the Spectral energy distribution measured in a structure for two different frequency ranges: Lower range (0-10Hz) on the figure (a), and higher range, until 100 Hz on the figure (b).....	11
Figure 13: Example of solutions found for 24 positions measured, where the best dispersion, which corresponds to the statistic solution, is equal to 0.03Hz for 17 modes found.	15
Figure 14: example of automatic extraction results of one FRF, for a vertical output accelerometer on the deck.....	16
Figure 15: Example of table of the frequency, damping and dispersion for each mode found and for two different types of output transducer.....	16
Figure 16: Example of mode shape value calculation from the FRF complex representation at one position (p20) and for the mode m (red symbol).....	17
Figure 17: mode shape of a flapper mode of the bridge edges in Y direction.	18
Figure 18: example of mode shapes of the same bending mode (no: 1) measured from acceleration above, and from displacement below.....	19
Figure 19: mode shape of the second bending mode (In “free free” condition) measured in acceleration	20
Figure 20: Rigid body mode shape of the deck on the elastic supports	20
Figure 21: Main torsion mode coupled to a flapper mode of the deck. From acceleration measurements	21
Figure 22: Case of high coupling between modes (bending 1 and flapper modes) giving not accurate damping values.....	22
Figure 23: global damping evaluation by the envelopes decay fitting, on a filtered signal of acceleration.....	22

Modal Analysis of Small & Medium Structures by Fast Impact Hammer Testing (FIHT) Method

1 Introduction

The Impact hammer test is currently used on small structures with little damping (steel structures) in the mechanical field. It is less usual for civil engineers to use this method to characterize the dynamic properties of buildings, frames or bridges probably for the large dimensions, and often for the damping of some of the materials and particularly for old structures. Another reason is the tedious analysis which is necessary to obtain meaningful and accurate results without errors due to instrumentation and data processing.

Since the method works at low level of energy, large dimensions and important damping are not recommended for this use, but nowadays with the quality of the transducers and with adequate signal processing, small and medium structures could be easily investigated. It is the case of most of the structures tested in the civil engineering laboratories.

One of the aims of the project SERIES¹ (task 2.3 “*software development for data processing*”) is the availability of simple tools and techniques for real-time data analysis and interpretation. The introduction of the Fast Impact Hammer Testing (FIHT) method takes its place in a field not yet covered by the different partners. Moreover, the objectives are to give the opportunity to the partners to use the method for a final insertion as a part of a set of toolbox built by the team of the Laboratório Nacional de Engenharia Civil (LNEC). The method will be used for the dynamic characterisation of some of the structures built for the SERIES project.

The main differences, between the classical impact hammer method and the FIHT described here, is that this last enables to get results in a very short time without reducing the accuracy.

The FIHT method has been tested on different structures, and the results were compared with those coming from commercial tools or algorithms developed at ELSA, and used for tests described in bibliography ([1] [2] [9] [10] [11] [20]). The result comparisons have shown a good agreement with the FIHT method.

The signal processing which is part of the FIHT method is implemented under Matlab and requires the installation of the correspondent FIHT toolbox. To be used without restriction it is necessary that the tests data are written in a readable format for Matlab.

2 The Fast Impact Hammer Testing (FIHT) Method

2.1 The reasons to develop the method

The FIHT (Fast Impact Hammer Testing) developed here can give a solution to find economically, quickly, and accurately, the main dynamical properties governing the behavior of small and medium structures.

It cannot substitute the commercial tools, rigorous but complex and expensive, used to characterize the dynamic properties of structures. However it brings an efficient support, to most of the needs in the dynamic field in civil engineering laboratories, because of its high degree of automation of the procedures.

The method briefly introduced here, is more detailed in the following paragraphs on an example of a structure tested in ELSA², to highlight the capacity and the advantages of the method, but also the drawbacks.

¹ SERIES: Seismic Engineering Research Infrastructures for European Synergies.

² ELSA: European Laboratory for Structural Assessment.

The structure tested is a fibre composite beam of 13 meters long, built for the European project named PROMETEO.

2.2 The differences between the FIHT method with respect classical Hammer methods

As the FIHT belongs to methods where the input is measured (here the hammer load), the results representation is mainly done using the transfer function (FRF) process between the input and output. The output could be measured by accelerometer, velocity, or displacement transducers at the own choice of the engineer. The main difference in the testing procedure with respect the classical hammer impact method is the extensive use of the reciprocity of the FRF which conduct to use one or two output only (instead of an important number in the classical method) and by consequence the absence of calibration tests.

The signal processing is performed step by step in an automatic way.

Several assumptions and criteria governed the acceptance to the next step. Some of them, mainly in the process of modal parameters extraction, are results of statistic procedure, and some from experimentation observations. The main criteria to validate the results are the used of the coherence function in a very compact form, which simplify the task without disturbing the signals content.

The main assumptions in the chronologic process are:

- The FRF noise level: defined by default from dynamic testing of more than 30 different kinds of structures, and materials for civil engineering. (It can be changed by the operator).
- The accepted coherence threshold value. Defined as previously (It can be changed by the operator).
- Damping and frequency values extracted from the FRFs are interpolated, and magnitude balanced, in the half power band method used for the automatic extraction.

The main limitations other than the structure dimensions and the input energy, is the validity of the transfer function reciprocity property used to fasten the measurement process which in some rare cases could be not verified, when by example bolts in steel structures are not well connected.

The second important inconvenient could be the incapacity of the modal extraction procedure, based on the peak peaking method, to isolate modes very closed, leading to operational deflection shape instead of pure mode shapes.

3 Structure Description and Methodology Employed

The illustration of the method is proposed here in an example of medium structure dimensions, built with both classical and new type of materials, namely concrete + composite fibers. As the structure had rather small dimensions and weight, the faster and most efficient method to get accurate results on the dynamic behaviour of the frame, was the use of the FIHT method.



Figure 1: General view of the structure on left and input (Hammer) and output (Accelerometer) transducers used for modal testing

Before starting the measurement campaign it is helpful to make a quick evaluation to understand if the hammer Impacts will be sufficient to excite the main modes of the structures. It can be done calculating the ratio between the dynamic impact force (measured) to the weight (force) of the structure tested. A ratio greater than 0.1 to 0.5% should be sufficient to expect adequate results. In our case a typical ratio is about (6000 N / 310 000 N) ~1.94 % and therefore the FIHT should be well adapted.

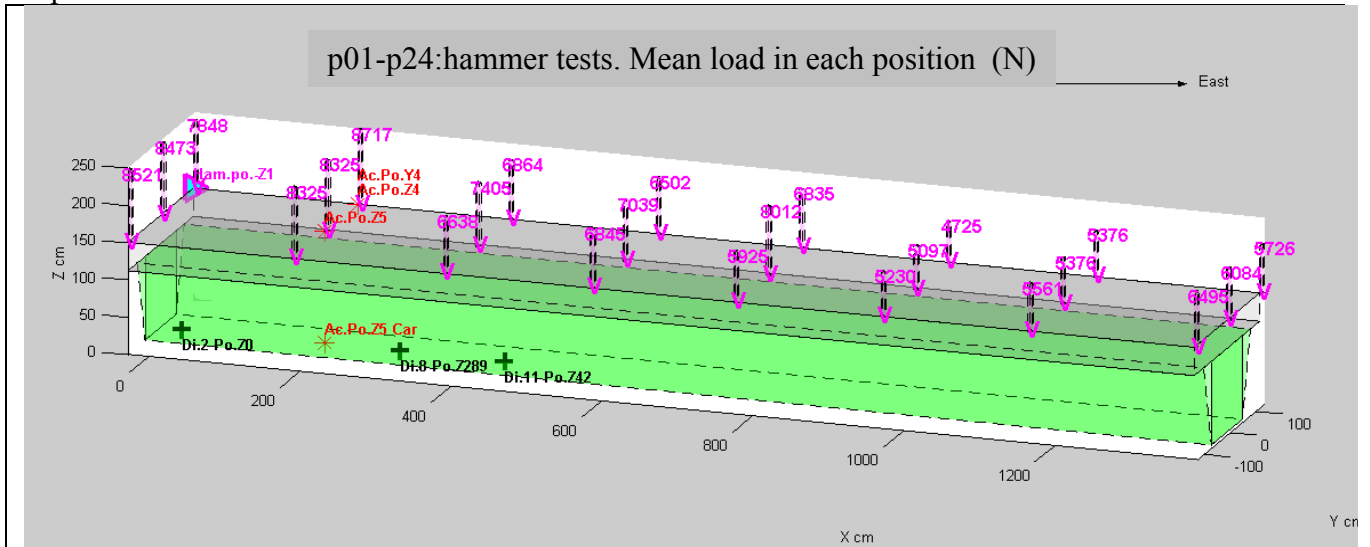


Figure 2: Structure design with the output transducers positions (red -black), and the map of the inputs (Impacts).

The structural excitations, is given by an instrumented hammer for which the impacts generate transient signals, characteristic of the frame tested.

In the present case the number of output transducers recorded for the dynamic tests of the structure is seven (7 channels).

With the FIHT method we need theoretically only one output transducer, but in our case as the structure was already instrumented for static tests, a total of seven output transducers (3 displacements + 4 accelerometers) in different places of the structure were recorded to acquire more information on the dynamic behavior.

The data of the table below, with exception of the point's number, are inserted before the test starts, for an automatic plot of the mode shapes.

For each test, each signal is recorded on a single channel which corresponds to one file. The filename in the example has the following mean: P12 is the test number, the following two digits (01) is the impact repetition number, and the last digits (01: to 07) is the transducer number.

Filename, Nb. of points	Transducer	Position	Unit	Coordinates
p120101	10104	Acceleration Ac.Po.Z4	m/s/s	190 126 150
p120102	10104	Acceleration Ac.Po.Y4	m/s/s	190 126 150
p120103	10104	Acceleration Ac.Po.Z5	m/s/s	190 0 150
p120104	10104	Acceleration Ac.Po.Z5 Car	m/s/s	190 0 0
p120105	10104	Displacement Di.2 Po.Z0	mm	0 0 0
p120106	10104	Displacement Di.8 Po.Z289	mm	289 0 0
p120107	10104	Displacement Di.11 Po.Z42	mm	428 0 0
p120108	10104	Force Ham. po.-Z12	N	585 126 150

Figure 3: Example of test description including the channel attribution and transducers coordinates.

4 The Fast Impact Hammer Test (FIHT) Method Description and Limitations

The tests are similar to classical impact hammer tests, where several impacts, for noise reduction, at the same point are given to the structure, but for the FIHT only one output point is necessary. Each

point corresponds to a particular transfer function (FRF) of the structure. In the classical method the accuracy of the mode shapes is defined by the number of output transducers attached at different positions, which gives the number of FRFs measured. Here, each new impact position corresponds to a new FRF. As we need only one output transducer, the number of FRFs measured could be greater, and then the geometrical accuracy of the modal shapes is also increased.

It is important to highlight that calibration tests are not needed as theoretically it is the same output transducer which is used for all the tests. The possibility to obtain each FRF in different measurements performed not in simultaneity is given by the property of reciprocity of the transfer function with respect the excitation point. The reciprocity is available only if the tests reach very small level of strain or displacement to remain in the elastic field, and deal with linear dynamic behavior of material and structure assembly which is the case of most of the new structures built actually. It is less true in the case of masonry and still worst in the case of old structures.

Even when performing several impacts in different positions seems a long operation, practically it is much shorter than installing the same number of transducers as impact positions. Pasting, calibrating and adding information in the setup to process the signals for each new transducer takes time and the number of on hand transducers is generally limited. It is in this experimental part that the main shortening is won by the FIHT method.

Each impact positions (Input position) will therefore corresponds to the nodes of a mesh where the FRFs are measured. It is of crucial importance in the method, to define the best position of the output transducer as it is a single output only. This point is discussed in the following paragraph. It could be necessary, in some cases to suppress some doubts, using a 2nd or a 3rd output transducers, to avoid some mistakes in the modes definition. The work is very limited as it is only one or two channels added to the recording system, even at the end we have most often redundancy of the results which gives a cross check between tests.

In our case the output is a capacitive accelerometer attached to the structures, where the amplitudes of the signals should be maximal for all the expected modes (in our case we want to measure the first 6 bending modes in the vertical direction of the bridge).

As the main aim of the tests is to obtain the modal shapes of the structure tested, one of the limitations of the method actually is the representation of the shapes in the 3 directions coupled, as the software is still not achieved. We can have the display of the motion only in one direction at time.

Another limitation could be the presence in a structure of material or particular devices, which do not respect the reciprocity of the transfer function. It is the analysis of the structure, which will prevent the use of only one output. In that case the method can be used, starting directly from the FRF recorded from simultaneity of the measurements (multi output). We have to paid attention to perform a calibration test before, as is usual with other methods.

4.1 Importance of the output transducer position

Generally a numerical model of a structure doesn't always give the correct values of frequencies and damping, but rather good design of the mode shapes. Then from the numerical mode shapes one can define the output position where the signals are significant for the mode expected (rejection of node positions). In this example, instead of modeling the bridge mode shapes, and assuming that the structure is similar to a beam simply supported, for the bending modes, the best output points are calculated analytically. The curve below shows the calculated results for the best placement of the output transducer. It corresponds to the highest level of amplitude we can measure for all the modes requested. The smoother will be the sloop around the peak found (as pointed by the black arrow on the Figure 4), the smaller will be the error on the transducer position.

Two maxima at symmetric positions are solutions. The position adopted is at a distance of 1.9 m or little less, and is the output reference accelerometer. Other accelerometers are placed at this abscissa position, in different places, to capture information from the other part of the bridge.

The analysis to find the best output for the FIHT method, or the best input for the classical method (which use a set of output transducers), is common to the two methods, but is very important to define it, in the case of the FIHT method as generally one transducer only, is used for the output. Having

define the placement of the transducers, and given that some other transducers (displacements, red stars in the Figure 4) are already existent for other purposes it is important as the structure is mainly composed of two parts, the deck and the carbon beam, to compare the output for each part, which conduct to add an accelerometer on the carbon beam.

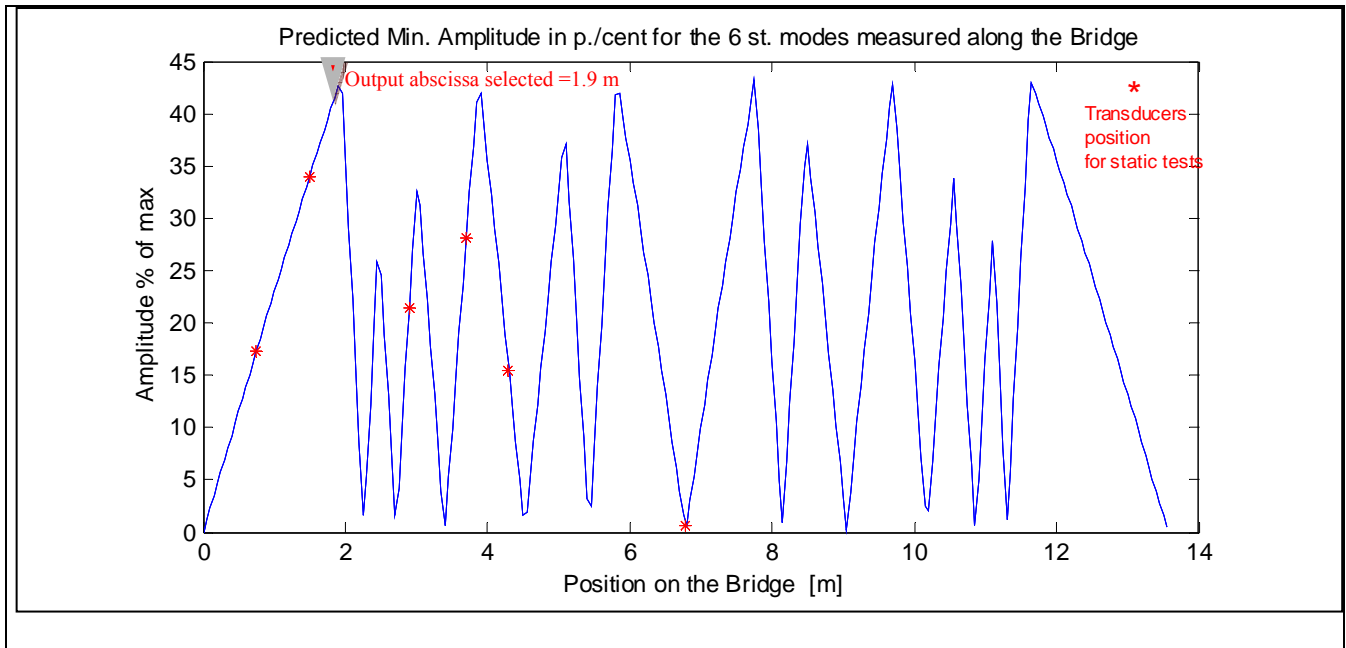


Figure 4: Analytical results to find the minimum amplitude of the first six bending modes expected along the beam

4.2 Remarks on the different steps when using the FIHT

If the toolbox of the FIHT, running actually under MATLAB, can read on line the signal time history of the tests, then a figure similar to the Figure 2 will be generated and modified on line. If it is not, as it is more often the case, the processing is performed at the end of the tests.

The total number of transducers for this example for each test is 8: 4 accelerometers, 3 displacements, and the input load given by the hammer. The coordinates of the transducers and of the impact positions (FRF) are defined before the tests starts.

The design of the structure at rest, in that case the bridge, is also define before the tests, in a MATLAB file with simple functions (see annex 1: 'beam', 'irbeam') which could be inserted in a toolbox to ease the display of a simple schema of the structure.

If all these data are inserted before the tests, the figure 2 will be automatically generated without the arrows.

After each impact test the arrows are plotted until they cover the total area measured. It is also important to note on the Figure 2 that the position of impacts (24), in pink, cover all the area of the deck, in a regular geometry, even each elementary mesh is not square. Each position corresponds to a FRF, each one being a mean of 5 single impacts. The mean load intensity is also mentioned by a correspondent pink arrow length on the slab.

In parallel of the figure 2 others figures are displayed which the understanding is given in the following paragraph, as they belongs to field of signal processing.

5 Signals Processing

5.1 General schema

As the energy inserted to excite each mode of the structure is very small because the hammer excites the structure on a large band of frequencies, where all the modes are equally excited, noise is always

present in the signals. Means, in the frequency domain, of the same measurements are very efficient to remove it. A short pre-test on the structure shows that in that case, five means are sufficient to cancel the noise efficiently. The total number of signals generated by the impacts for testing all the structure is important and equal in our case to:

5 impacts x 24 positions x 8 (output +input) transducers = 960 signals. !!!

Because all of them contribute, in a small part, to define the correct modal parameters values, an automatic signal processing is mandatory to check in a very few figures the validity of the overall signals and the transducers operation.

To understand the automated signal processing, a view of the main operations between the recorded signals (1st column) to the final results (last column), is displayed in the Figure 5. It shows that for each point p of the structure tested (each FRF) at least 2 signals (1 input + 1 output) is measured n times (n=4 to 10).

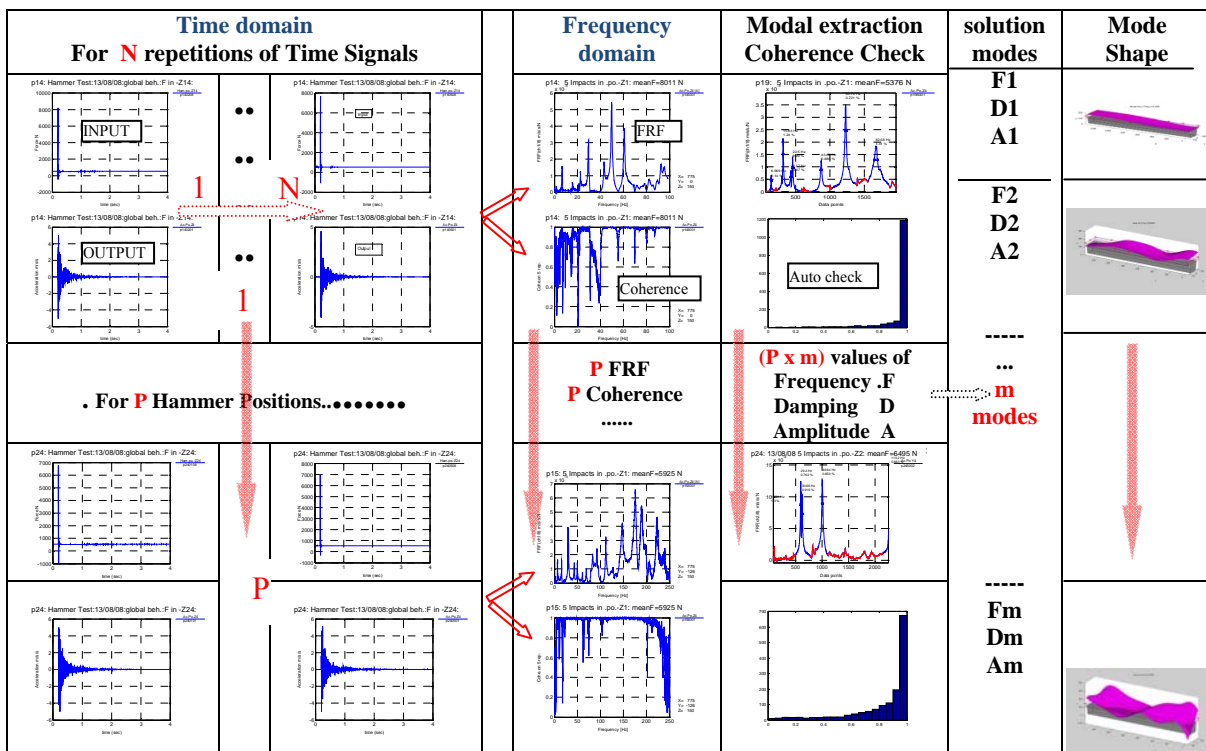


Figure 5: Processing time signals and frequency analysis for modal extraction by the Fast Impact Hammer Testing (FIHT)

From the time signals (n input +n output) at the same position p, a transfer function is computed (with or without windowing), giving a mean spectrum of the p measurements in the frequency domain. From the p FRF, m modes are extracted, which have their own properties which are the final results: Modes frequency, modes damping and modes shape.

In this example as 24 points are tested we obtain 24 FRFs, means of 5 repetitions each.

As all the operations are performed automatically, before extracting the modal parameters from the FRFs, it is necessary to check if the measurements and /or the transducers work.

The displays of 960 time history signals, for this example, which is common for a structure of these dimensions, is not really adapted for the time needed to inspect each of the signals. Furthermore, even the time history shows that the transducers are working, it cannot show the correlation between input and output.

The solution adopted here is an automatic check of the signals, illustrated in the following paragraph, and performed using an adapted display of the coherence, a function well known, in the field of the dynamic testing.

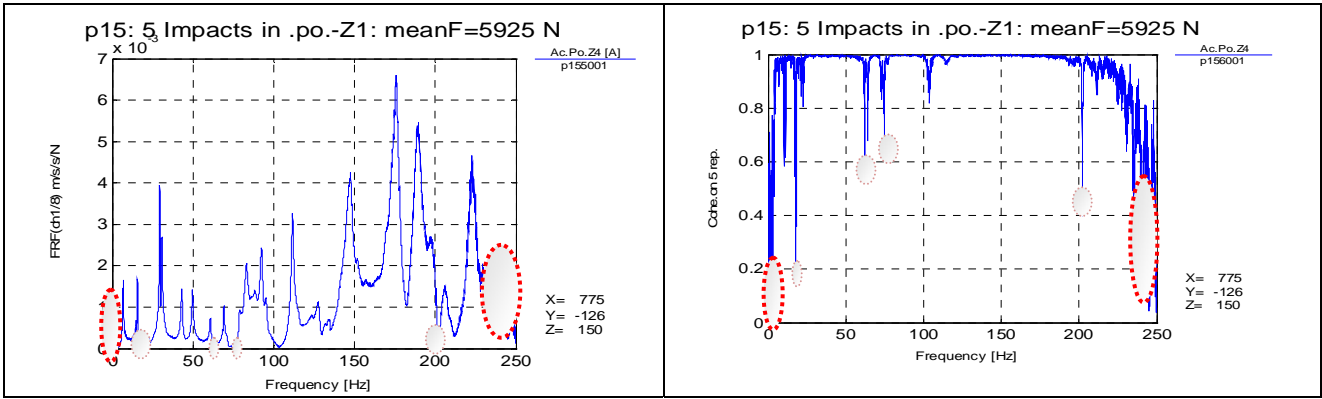


Figure 6: example of the mean FRF of one point position on right, and on left the respective coherence function of the same set of measurements.

For each FRF the coherence function calculated, which is a statistical function, show how much the output is connected to the input on the frequency band inspected. A value of 1 corresponds to a perfect correlation between the impact and the output signal measured.

On the Figure 6 an example of a FRF and its respective coherence function is plotted. It shows how the human eye can understand easily if the measurement is correct but how is difficult to find a criteria which eliminate erroneous measurements.

On the Figure 6 low values indicated by circles indicate problems in the measurements. The pink circles are only problems of signal/noise ratio which can be removed by FRF filtering as explained on the next paragraph. Red colour of the circles are real problems which are not removed by the automatic check. It represents on left, the cut off frequency of the hammer (at very low frequency), and at right the filter of the acquisition system which was chosen at 200 Hz for these measurements. It is then normal that the coherence values included in the red circle are taken for the processing as they show a real problem.

5.2 Automatic Check of the Measurements by Coherence Histograms

For a modal test as the bridge example here described, we have measured 24 FRF for each Output transducer (7), which corresponds to (24x7=168) figures of coherence to be observed. It is a very important time cost. In the FIHT we proposed a shortening of these operations, condensing the information in two check levels.

The first is the histogram representation of the coherence function dividing the coherence values in bins (default=20) and displaying the histogram of the points distribution for all the Output transducers (OT=7) on the same graph as it is shown on the Figure 7.

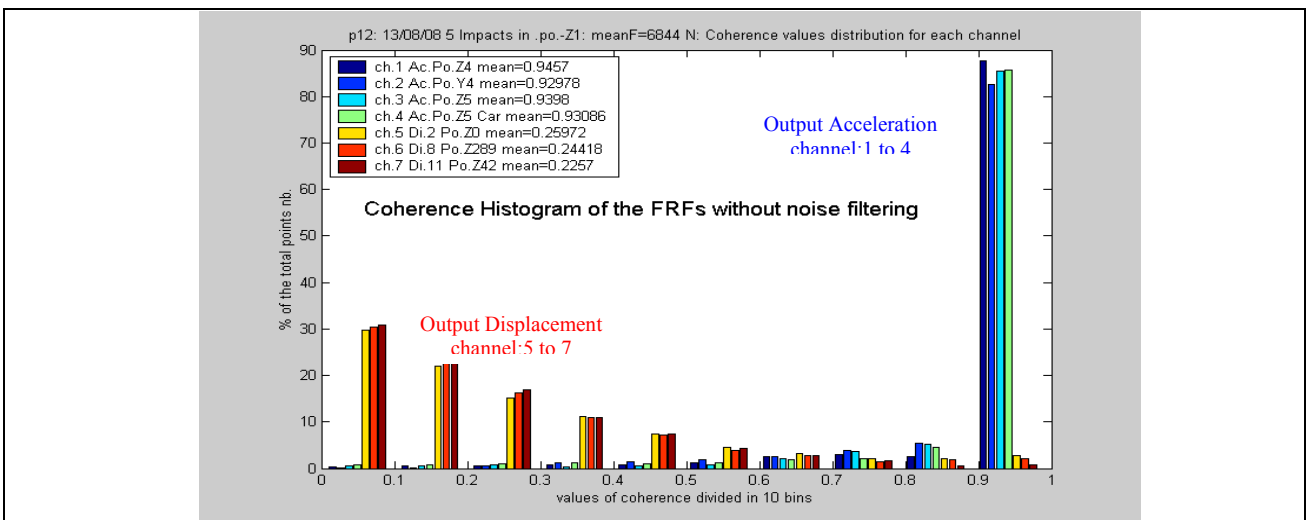


Figure 7: Coherence histogram of the FRF on row data, and for one position. One colour by output transducer.

With this operation we divide by OT (7 in this case) the number of graphs to be observed, and in the same time we quantify the validity of the measurement by a number (mean value of coherence) and a histogram distribution (positive exponential, flat, etc... distribution).

It is interesting to observe that at the point position tested, the distribution and the mean values are very different between groups of transducers; one with 3 displacement transducers, and one with 4 accelerometers. With this example, we highlight the fact that the hammer induces very small deformations on the structure but not obviously inaccurate displacements.

This remark, conducts to process the FRF and coherence files as it is described below, to obtain a reliable check by the coherence function and explains why the direct coherence is not used.

The above histogram shows that for displacement FRFs, the mean values are far from 1 (0.22 to 0.26) and can indicates to the user a problem in the measurement or in the transducers. A plot of the time signals and of the processed results of the FRF and coherence in the Figure 8, helps to understand that the very small modal density (3rd graph) of the signals is responsible of the low mean value observed in the coherence histogram, even the transducers works, and the output signal is correlated to the input given by the hammer.

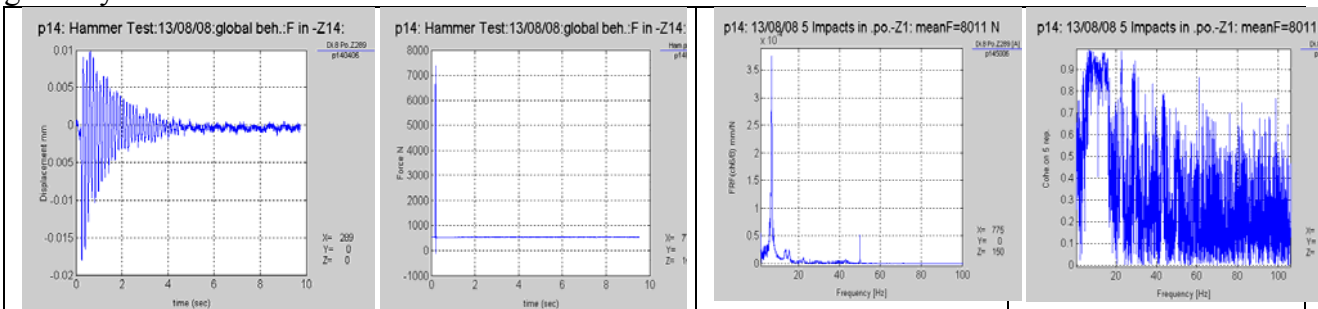


Figure 8: From left to right, example of displacement and force time history with relative FRF and coherence.

Coherence histograms made on row data are not always adapted to perform an automatic processing. Processing raw data could conduct to discard measurements which are not erroneous. From the example above we can understand that only the part of the FRF with high signals-noise ratio (where the modes are present) have to be taking account in the coherence histogram processing.

In the FIHP method, points with level lower than three orders (default) of the maximum magnitude of the FRF processed, are removed because they represent measurements highly affected by noise and therefore with poor coherence. This step achieved (automatically in the FIHT), processed data of coherence could be submitted to a statistical criteria which enable the user to accept the measurement:

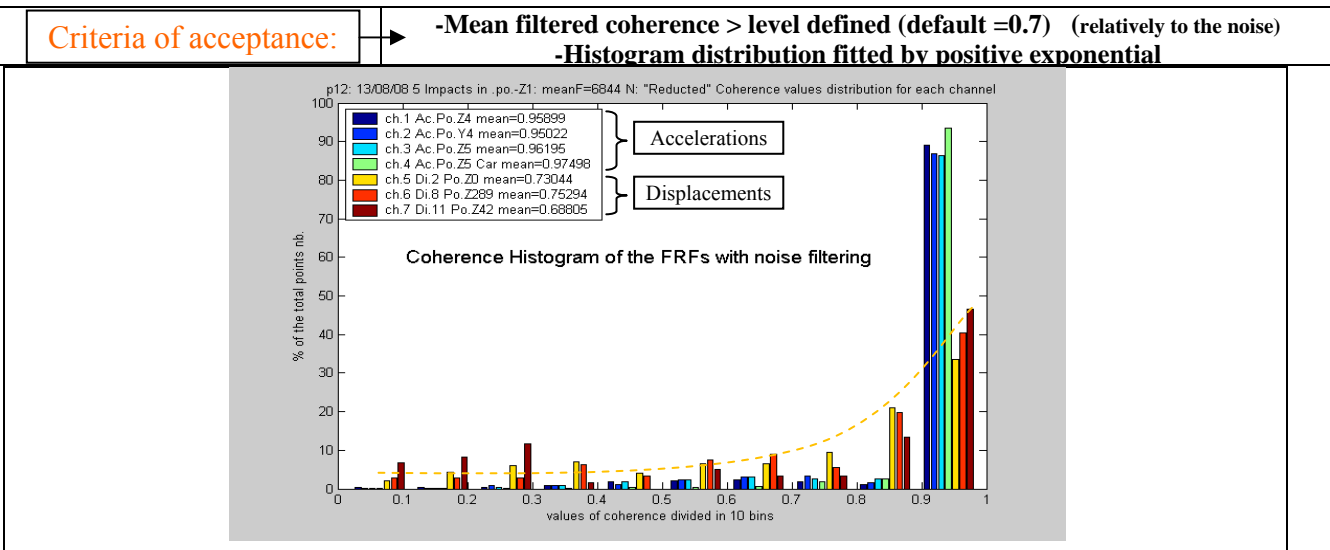


Figure 9: example of distribution of the coherence values for one test (5 impacts) and for all the transducers.

Now the filtered coherence histogram has the appearance of the figure above. It shows that the criteria is respected for the acceleration signals, meanwhile for the displacements the mean values remained low (~ 0.7) but acceptable. It is a warning guiding the user to check time displacement signals which shows to be small, but not un-coherent. An increasing exponential shape could be now fitted to the data and the processing can continue.

A second level of automation could be performed to reduce in one graph the check of all the points' position tested (24 in our case). In the Figure 10, on the example of the PROMETEO beam, we show the spatial distribution of the impacts, where each stick length represents the mean of the filtered coherence. Each value upper the limit defined as a default threshold (0.7) appears in blue. The default value could be changed by the user, for particular reasons. Under the threshold value the sticks have an orange colour which help the user to understand where are the problems in the measurements.

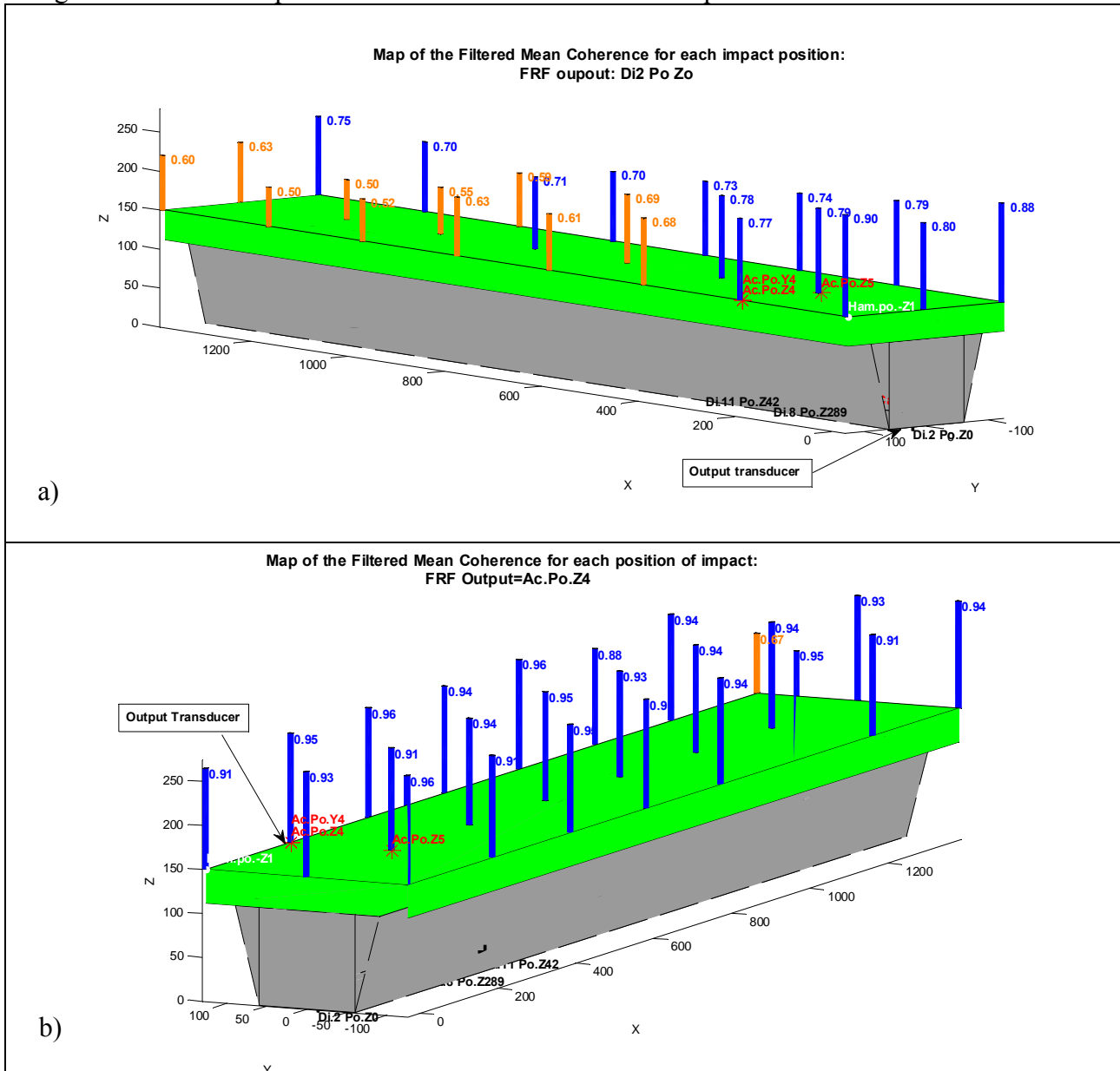


Figure 10: Example of the map of the filtered coherence for 2 types of transducers: displacement (a), and accelerometer (b).

In this way the user can understand quickly the overall tests validity. On the Figure 10 (b) the values of coherence show that the accelerometer FRFs are of good quality with the exception of one side point (value of 0.67) probably due to a wrong impact (among the 5 ones). The user can then verify for this position if one of the five time signals has to be rejected.

On contrary on the Figure 10b the coherence values are much lower showing therefore poor signals for the FRFs displacement, but in the same time the space distribution brought the following information: farer is the impacts from the output transducer, lower is the coherence value. The coherence map indicates, in that case that it is a problem of level of energy.

Concluding the problem of coherence analysis, on the example, we can say that seven histograms + seven maps (for each output trans.) are sufficient to understand the overall validity of the 960 signals.

5.3 Maps of the FRFs amplitude

The last step of signal processing, before the modal parameter extraction, is the representation of the FRFs amplitude in the direction of the motion measured. Depending of the type of transducer used for the output, the magnitude represented could be in displacement, velocity or acceleration. As the FIHT method used mainly the hammer impact for input, the level of displacement generated are small and it is rather convenient to represented (after measurements) the acceleration FRFs to get visible also the mode shape of high frequency.

In a first step the program displays simply the FRFs magnitude of the ten (could be changed by the user) positions which have the highest level of signal (spectral energy) in the total frequency band analysed. The plot of the curves in 3 dimensional graphs helps the user to understand if the FRFs magnitudes correspond to physical results expected.

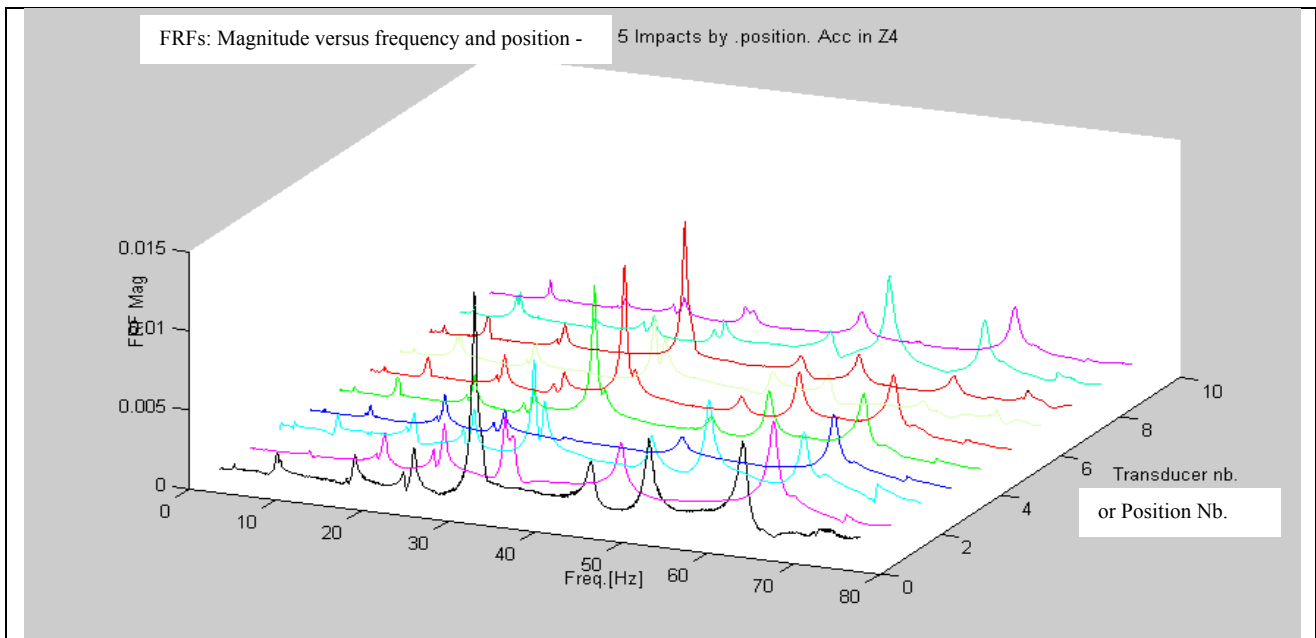


Figure 11: Example of FRFs magnitude of the test no: 1 to 10 (5 impacts each) and acceleration measured in position Z4

It is important to have a global displays of the curves, as from each of the single FRFs are extracted the values of the frequency, damping, and mode shapes (for each of the modes excited).

Another way to read the curves for an easier meaning is also to represent the level of spectral energy distribution in the structure in a defined frequency band. The map of the spectral energy is automatically plotted for the output transducer selected in the frequency range required. The result, plotted in the Figure 12, shows the map of the level of vibration in the structure allowing quick displays of the points of the structure mainly excited in a range of frequency. The dynamic behaviour is then easier to understand by this kind of mapping. It is important to note that the results will also depend from the position of the output transducer. In effect even the force variations of the impacts are taken into account in the FRF measurement, the amount of energy dispersion in the material increase with the distance Input-Output. Therefore the interpretation of these maps has to be done with care if the material is dispersive or if the structure is old. In effect in that cases the FRFs magnitudes measured ($||mesFRF_{ij}||$) must be multiplied by an exponential coefficient of the type:

Equation 1:
$$\|FRF_{ij}\| = \|mesFRF_{ij}\| \times e^{d(\alpha + \frac{\omega}{c})}$$

Where:

- i is the input position and j the output position.
- d is the propagation distance of the wave between point i and j.
- α is the attenuation coefficient of the material.
- ω is the angular frequency.
- c is the wave velocity in the material.

For steel structures this coefficient could be neglected. We can note that in the formulation above, in the case of collocated transfer functions ($i=j$) the exponential term is equal to 1 because the distance d between i and j equal to zero.

The maps shown on the Figure 12 are calculated from each of the FRFs experimental magnitude, using the Delaunay interpolation on the surface and direction of the impact measurements, and represented by a colour proportional to the spectral energy value.

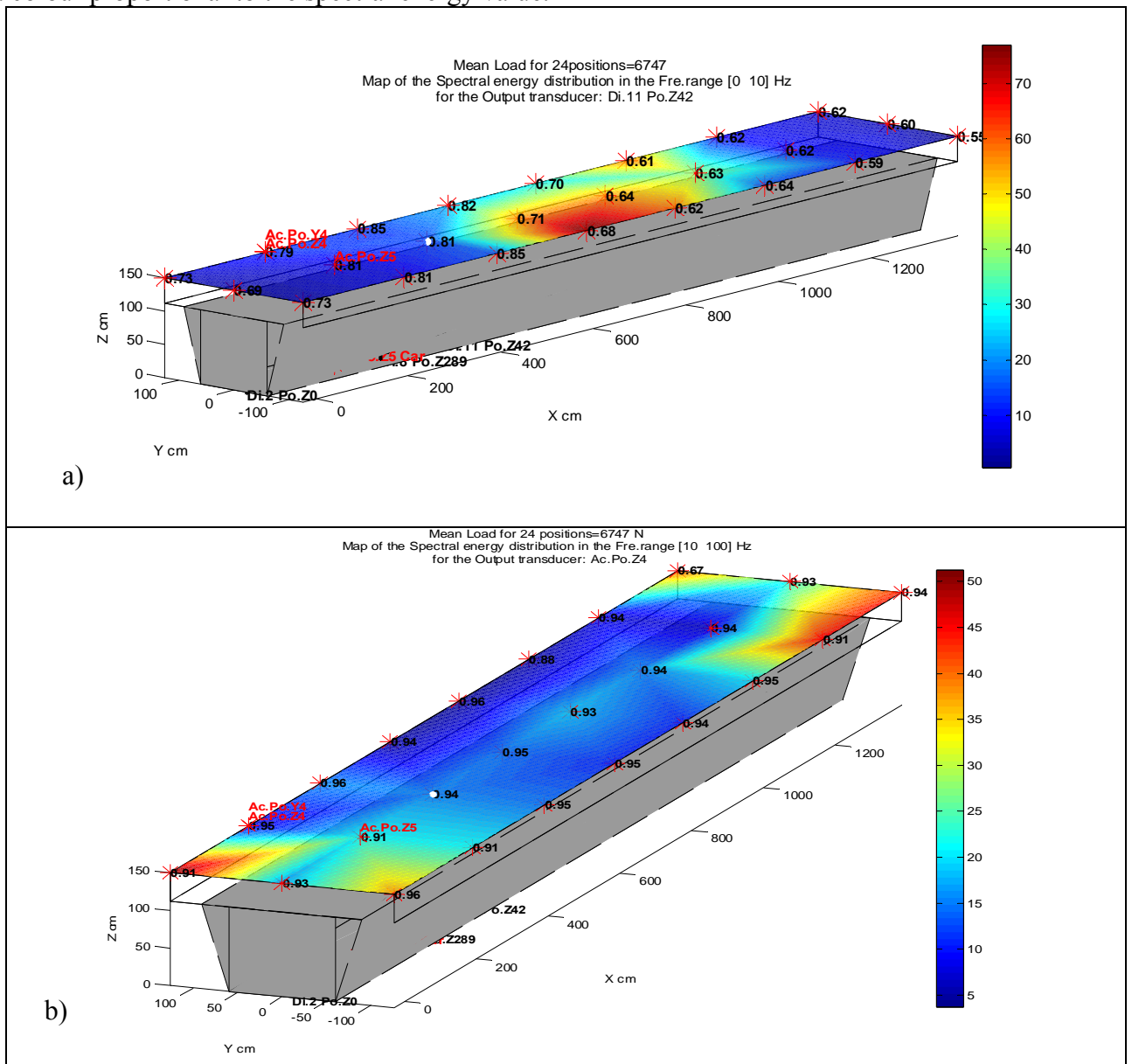


Figure 12: Example of maps of the Spectral energy distribution measured in a structure for two different frequency ranges: Lower range (0-10Hz) on the figure (a), and higher range, until 100 Hz on the figure (b).

On each point measured the filtered mean coherence value is reported to help the user to identify a measurement problem or a true physical behaviour. The spectral energy mapping is useful for the structural designer which can understand the region in a structure, which will reach high level of strain from the FRFs displacement (Figure 12 a), and high level of acceleration from the FRFs acceleration (Figure 12 b). It shows the critical zone of a structure subject to a specific frequency range of dynamic loading. Practically who use the FIHT method, has only to choose the output transducer and the frequency band to display one map.

6 Modal Parameters Extraction

6.1 Principle of the fast extraction used in the FIHT

Even it is not the aim of this report to give the methodology of the modal parameters extraction, to understand the fastening brought by the software part of the FIHT, it is necessary to explain the principle of the modal identification used here and described in the next paragraphs. Other information could be found in reference [1] and [2]. Only some examples of results are presented in the following paragraphs, which corresponds to the main identified modes, and to highlight the performances of the FIHT in a practical example.

The extraction of the frequency, damping and amplitude is performed in the frequency domain by the implementation of a routine based on the Peak-Peaking method [3] [4], and modified to fasten and accurate the procedure. The main modification is coming from experimental evaluations, which shows that the higher is the peak amplitude, the more accurate will be the frequency value of the mode. This remark conducts to balance the frequency values by the amplitude level of the peak, to obtain the mean frequency value, coming from the different positions measured.

As the aim of this method is to obtain a quick overview of the experimental modes, therefore there is not a FRFs curve fitting tool [5], and neither a Modal Assurance Criteria (MAC) [6], to fasten the processing. The modes are found by empirical statistic criteria based on the dispersion of the frequency values for all the modes and positions measured.

- First, the user selects a number of modes (N_m) to be found. The N_m higher peaks (not spurious) are then selected in each FRF, automatically.
- For each peak the modal parameters (frequency, damping, and amplitude) are extracted from the magnitude and the imaginary part of the FRFs by the software. We obtained a set of frequency, damping, and magnitude values.
- To select the frequency values which belong to the same mode and therefore to find the correct number of modes, the parameter to be optimised in the method is the frequency dispersion. Because the frequency values obtained from measurements of the same modes, in different positions are rarely exactly the same (for different reasons explained in [1]), and sometime in such position (node) they don't exist, a statistic procedure is used to calculate the best frequency dispersion (bdf) giving the optimal regrouping of the values. The procedure is explained in the following paragraph.
- The limits of the frequency dispersion (df_{\min} and df_{\max}) are defined below.
 df_{\min} is the result of a calculation meanwhile df_{\max} is a value defined by the user, but by default corresponds to a mean value resulting from the signal processing of about 30 different structures
 $-df_{\min} = (1 / (10 * T_{\text{rec}}))$ where: T_{rec} is the total time of the signals record and 10 is the interpolation points number of the sampling frequency around each peaks. It is then equal to the frequency resolution divided by the interpolation introduced in the modified peak peaking method.
- $df_{\max} = 0.05$ Hz by default and can be changed by the user (decreased for mode coupling, or increased for noise in signals or FRFs).

6.2 Criteria for optimal grouping (= solution)

The solution is the ratio of a statistical (for F1 definition) and empirical (for F2 definition) functions. It consists in finding the groups of frequency values (modes) from P (positions) different FRFs. Each group m_i should be one mode of the structure tested.

For each frequency dispersion df_i exists a frequency matrix MF_{df_i} of P lines and m_i columns. If in one position (=FRF) there is a node for one of the mode, on this FRF there is no peak in correspondence. Then in the matrix MF, in the line corresponding to that FRF and in the column of this mode it will appear 0. The total number of frequency matrix considered is equal to (df_{\max}/df_{\min}) . The solution consists in finding the best frequency matrix between the set of matrix define below:

$$\text{Equation 2:} \quad \left[MF_{df_i}(p, m) = f_{p,m} \right]_{df_{\min}}^{df_{\max}}$$

Where $f_{p,m}$ = frequency value at the position p ($1 < p < P$) and for the mode m ($1 < m < m_i$). The total number of modes found m_i is dependent of the frequency dispersion value df_i .

To reach the best regrouping (best frequency matrix), the software minimises the ratio of two functions F1 (df_i) to F2 (df_i), which exist in the interval $[df_{\min} \text{ } df_{\max}]$ and are defined below.

Practically, F1 can be call the “minimum dispersion”, and F2 the “maximum stability”, and the solution will be the “**minimum dispersion for the maximum stability**”. We can note that the availability of the solution is relative to the number of the measured point number P. Higher is P more confident is the statistical solution.

The number of points of the functions F1 and F2 is then equal to (df_{\max}/df_{\min}) , because each value of frequency mode value cannot be smaller than df_{\min} .

F1 definition:

For each matrix MF_{df_i} , F1 is defined by the normalised sum of the standard deviations (std of matlab) of all the modes found together for the frequency dispersion df_i :

$$\text{Equation 3:} \quad F1(df_i) = (m_i)^{-1} \cdot \sum_{k=1}^{k=m_i} \sqrt{\frac{1}{P-1} \sum_{p=1}^{p=P} (f_p - \bar{f}_k)^2}$$

Note that F1 is in hertz and is calculated for each matrix MF (df_i) independently.

\bar{f}_k is the mean frequency of each group k (mode) of P frequency values.

F2 definition:

The function F2 is a step function and is dependent of several matrix $MF(df_i)$. Each step is the dispersion width where, if m_i is the number of modes for the dispersion df_i , $d(m_i) / d(df_i) = 0$

In other words, F2 is the length of the window dispersion from which the number of modes doesn't change.

$$\text{Equation 4:} \quad F2(df_i) = \sum_{s=1}^{s=Q} L_{A_s} \cdot \chi_{A_s}(df_i)$$

Where L_{A_s} is the length of the interval A_s and Q is the total number of interval ($Q < i$).

And

$$\chi_{A_s} = 1 \text{ if } df_i \in A_s$$

$$\chi_{A_s} = 0 \text{ if } df_i \notin A_s$$

Remark:

Equation 5:
$$df_{\max} - df_{\min} = \sum_{s=1}^{s=Q} L_{A_s}$$

Solution definition:

Having defined F1 and F2, functions of the frequency dispersion df_i , we can write the statistic solutions as call before: the “**minimum dispersion for the maximum stability**”. It corresponds to the sorted vector Sol where each element i is defined by the following ratio:

Equation 6:
$$\text{Sol}(i) = \max \left\{ \frac{F2(df_i)}{F1(df_i)} \right\}$$

Theoretically the vector Sol has i values which are the i steps of df_i . Practically the software display only the first three solutions (Sol(1:3)) as they represent the most probable best solutions (highest 3 ratios). If the function of the modal extraction is inserted in an automated loop, only the first solution (Sol(1)) is used.

6.3 Physical meaning of the functions F1, F2 and of the Solution.

It is important to remember that the solution in this method is statistic/empiric and that the greater is the number of measurement positions, the more accurate and realistic is the solution found. Therefore the solution is not exact but represents the closest frequency value of the mean experimental values taking account of the sampling, the interpolation and of the amplitude weighted.

It is not the result of an equation resolution but only the optima which verify the assumptions discussed in the following.

The understanding of the solution is illustrated here on the structural example which in this case is the results of a set of 24 measured FRFs with one output position (1 accelerometer on the deck of the bridge beam). Each measured FRF gives a set of (mf) frequency values.

Different values of peak frequency are measured for the same mode between each of the P positions (FRF) due to several reasons dealing with signal processing and structural behaviour. They are mainly:
 -the sampling and the interpolation of the mode peaks which gives different values but very close together (very small error).

-The amplitude differences of the same mode measured in different positions could bring an error on the frequency value even if in the FIHT method the frequency is balanced by the amplitude level.

-The highest frequency difference is probably due to the mode coupling when this last exists, but the error in this case is partially reduced by the amplitude level headed correction. In effect, even coupled, the modes of high amplitude are less perturbed (in frequency) by neighbour modes of smaller amplitude.

Given this distribution of frequency values, the objective is to find the different groups of 24 values by modes. At this aim we have chosen to use one statistic parameter which is the frequency dispersion (FD). If the FD is small we find a high number of groups (modes), but some elements of two successive groups could belong to the same real modes. It is, what is highlighted in the circle of the function F2 in the figure below. Enlarging the frequency window we can reach a stability in the number of elements by group which could be in our case of 24 or less in case of node position. It is the best arrangement in the probability sense. Enlarging the dispersion window, when the number of modes stops to decrease, it means that we are over the dispersion due to signal processing. We have reached the highest stability (step length). It is represented in the Figure 13 by the lower graph and the longer step of this graph.

This last parameter does not reflect the ability of the separation of close modes. We need to define a second parameter calculated in the function F1 which enables to minimise the errors due to problems of mode coupling. It is the standard deviation calculated on each group of frequency values and summed

for all the modes (groups). Smaller will be the normalised sum and higher is the probability that the grouping is correct, which means that peaks of the same mode belong to the same group.

The function F1 is shown in the above graph of the Figure 13.

As expected, the trends of F1 seems to be inverse of the step function F2; F1 increases because each single std (for each group) increases with the window width dispersion. F2 in the other sense will present always larger steps when the dispersion increases. Both functions F1 and F2 have irregular trends.

It is reasonable to think that the best solution will be:

- Close to the first point where begins one of the longer steps of F2 because up from this point the dispersion increment has no effect on the number of modes (grouping).

- at the local minimum of F1 in the interval A_s found with F2 .

A way to evaluate the optima of both observations for the solution is to calculate the highest ratio (F2/F1) which is the most stable configuration for the minimum local dispersion of the frequency values applied to all the modes processed. Both functions F1 and F2 are expressed in hertz, and the ratio is then dimensionless.

This ratio is also a curve with several peaks. The solution is the peak of maximal amplitude, but as it is a statistic approach it is important to consider the solutions represented by the others smaller peaks.

It is the reason why the representation on the Figure 13 shows the main solutions as red stars in the graph below of the Figure 13. The highest star is the highest ratio and then the best solution, but it is important to consider solutions which have ratio very similar even they have a very different value in dispersion. As actually the knowledge cannot allow to decide rigorously which of the function F1 or F2 is the most important it is suitable to compare the solutions. The comparisons have to be done in term of modes shapes. Generally the solution gives the same modes shapes. The user has then to choose the most regular one.

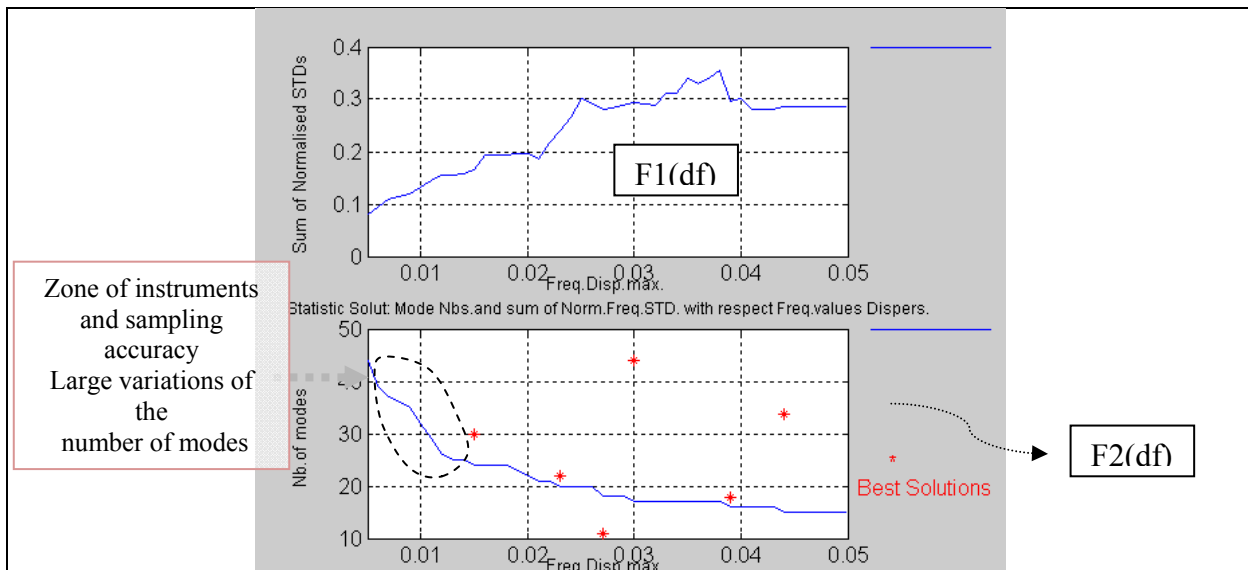


Figure 13: Example of solutions found for 24 positions measured, where the best dispersion, which corresponds to the statistic solution, is equal to 0.03Hz for 17 modes found.

Others details of the process could be found in [1]. In the Figure 13 are shown an example of solutions corresponding to the three dispersion values of the best solutions (maxima of $\{F2(df)/F1(df)\}$). The upper graph is the sum for all the modes of the standard deviation with respect the frequency dispersion (F1). The graph below is the number of modes found with respect the frequency dispersion, which helps to understand how is calculated F2, but it is not the graph of F2, and shows that from particular values of dispersion the number of modes is stable. These points are candidate for the solution.

Then the user can visualise all the modes shapes for each solution found. Generally the first one is the solution chosen by the user.

6.4 Representation and results of the parameter extraction

An example of FRF identification is shown in the Figure 14 below. It could be seen that on each peak identified, the blue stars corresponds to the half power band values measured. Red parts of the curve are modes still un-identified, for their low level of magnitude. The user can force to access to the modes un-identified increasing the mode number requested.

The principle followed in this method is that the dynamic behaviour is nearly not affected by the modes of low amplitudes (red part of the FRF in the figure below), and then their contribution in the behaviour of the structure could be neglected. The method is oriented to practical applications.

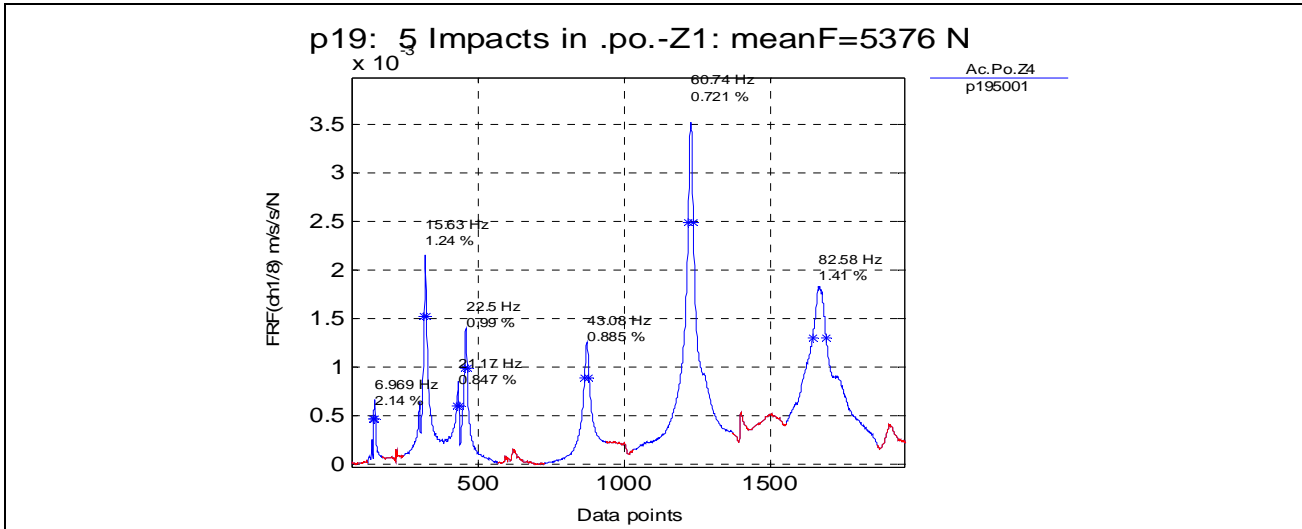


Figure 14: example of automatic extraction results of one FRF, for a vertical output accelerometer on the deck.

After the automatic identification process all the FRFs are plotted with the value of frequency and damping of each peak as it is shown on the figure above. An example of results after the complete processing is shown in the table below which corresponds to the combination of 24 FRFs and for three output transducers only (3 columns). Each sub-column corresponds to one modal parameter:

The first is the frequency, then the damping and the third the maximum dispersion of the frequency value for the mode found (simpler but similar to a classical Modal Assurance Criteria value). Smaller is the 3rd parameter and more confident is the results found.

Central Displacement Middle span (Vertical. Direction)			Acceleration.Po.Z4 South edge (Vertical. Direction)			Acceleration.Po.Z5 central on carbon beam (Vertical. Direction)		
2.2427	3.8139	1.7728	6.6333	5.6782	3.2746	6.9415	3.4977	1.0762
6.913	3.8294	0.9527	6.9685	3.6738	1.6450	14.5682	2.5197	1.0582
15.5804	2.2164	1.3422	14.5915	2.3884	1.4881	15.6060	2.5747	0.9896
35.5708	0.2042	2.1082	15.6066	2.6047	1.3420	20.9835	3.3967	1.4146
36.5460	0.2346	2.3860	21.1717	1.7376	0.8944	22.4642	1.9404	0.4383
			22.4842	1.8966	0.5426	26.9951	1.0382	2.9244
			29.4690	1.5541	0.9104	42.9814	1.9092	1.1581
			30.6082	2.0741	1.3252	60.5290	1.6361	1.9965

Figure 15: Example of table of the frequency, damping and dispersion for each mode found and for two different types of output transducer.

It is interesting to note that the first mode of bending highlighted in yellow for the three transducers, has frequency values in well correspondence in each output transducer, and all of them give a high damping value with respect the other modes. It is an indication to the user that the mode is probably coupled.

From the redundancy of the measurements (3 outputs represented in the table), on the 2nd column the acc. Po Z4, it is clear that exists a mode close to the first bending, with a high level of damping (5.7%). It is important to note that the method identify modes distant of less than 5% in frequency, but cannot calculate the damping with accuracy. The mode shapes in Figure 17 and in Figure 18 will give the explanation of this high level of damping. The facility to obtain the modal parameters and the mode shapes allows, comparing in a quick time, the use of several output transducers together, for a best understanding of the dynamic behaviour.

7 Mode Shapes

7.1 Mode shape calculation

The final step of the method is the mode shape representation.

In the previous step we have extracted the values of the Magnitude $(M_{frf})_m$ and the Imaginary part $(I_{frf})_m$ for each value of the mode m identified. In the FIHT, each experimental points P of the structure, when subject to vibrations, for each mode m , takes the following coordinate at each time step t ,

With: $-1 < t < 1$ chosen for the mode shape animation.

$$P_{m,c}(t) = [\text{point coordinate at rest } (X_o, Y_o, Z_o) + A \cdot \{M_{frf} \cdot \text{sign}(I_{frf})\}_{m,c}(t)]$$

Where A is the amplification factor of the dynamic part (2nd member) of P .

The default value of A is 200.

Note that only one coordinate c is affected by the dynamic part, in this example but if measurements exist in others directions, the same calculation will be performed for the other coordinates.

On the Figure 16, the red arrow and point, shows which values are taken for the mode considered. All the information from the process of modal extraction is stored in matrix of Matlab. An example of the command of extraction is shown below and enables to understand how easy is the processing for the user which can change one parameter to get the results expected. The software line, which calls the routine of modal analysis, is shown below.

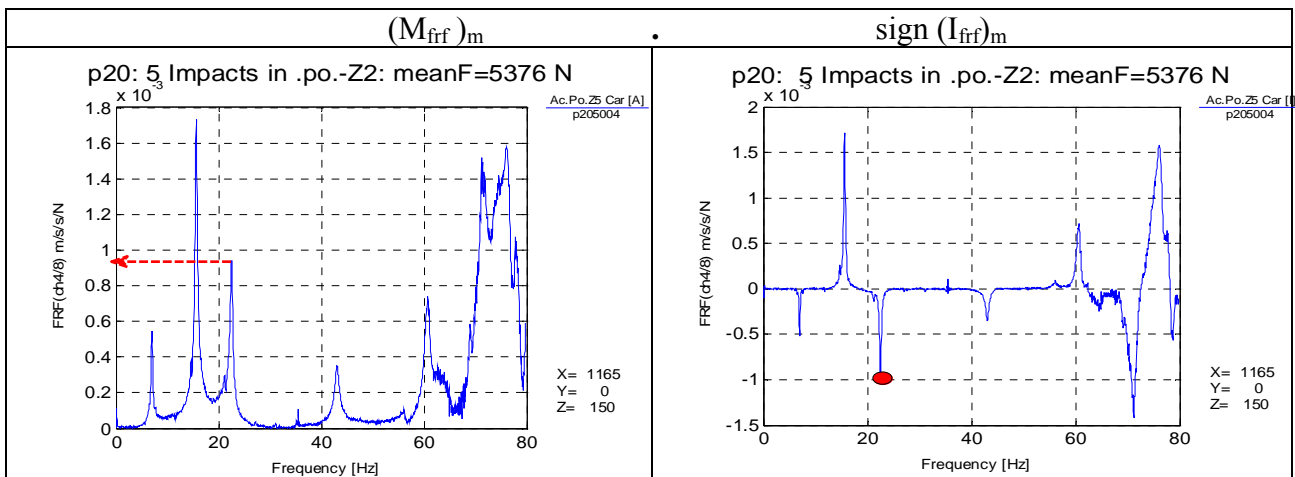


Figure 16: Example of mode shape value calculation from the FRF complex representation at one position (p20) and for the mode m (red symbol).

[NFR NDA NAM FRFP NCOL FDM]= modal(**Vec**,**Nbm**,**Crm**,Four,Fi);

INPUTS: (the 3 first are compulsory)

-**Vec**=list of FRF measured and stored in vectors,

-**Nbm**=nb. of modes searched in each FRF

-**Crm**= criteria on modes =in how many FRFs we expect the presence of the modes. In other words, peaks at same frequency(or nearly) are considered modes is they are observed in at least Crm FRFs or positions.

The following parameters are optional:

-Four= dispersion range requested in % if different of the default (= [0.1 to 10%])

-Fi= filter value (if different of the default, to extract, by example closed modes

(define in point number)

OUTPUTS parameters:

Matrix of Peaks frequencies (NFR), damping (NDA), amplitude (NAM), address (FRFP),

NCOL =nb. of the columns which respect the criteria Crm,

FDM=matrix of frequency damping and standard deviation of each mode found.

7.2 Mode shapes representation

To fasten the work for the user which have to design the structure, two simple functions (beam and irbeam) in matlab are implemented for the representation of the structure at rest (see annex 1). The display of the structure at rest and of the mesh of all the FRFs positions and surface, is, then automatically generated, if the coordinates and the direction of motion are previously inserted in a matrix of coordinates.

The program shows, by increasing values of the frequencies an animation of each mode shapes, moving the surface in the measured direction. As the mesh of the moving surface measured must be dense enough to produce accurate results (more than 900 regular meshes for each surface), the interpolation of the impact position is then irregular, and is computed by the Delaunay triangulation.

Different examples of mode shapes obtained by the FIHT method for this structure are illustrated in the following figures (15 to 19). All are pictures of the maximum curvature (the software stops its animation at this point and save the picture). They are amplified by a factor selected by the user (default=200 for a significant dynamic motion). During the processing, the mode shapes are animated and could be saved in "files.avi" format, or ".jpeg" for fixed image as below.

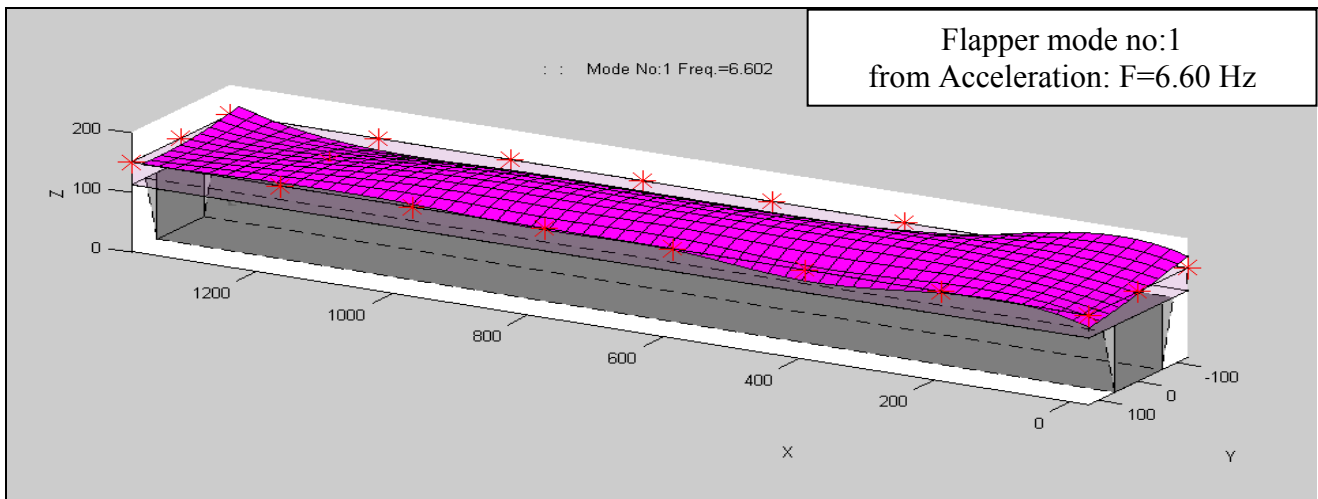


Figure 17: mode shape of a flapper mode of the bridge edges in Y direction.

It is important to note that the output transducer type, here an accelerometer, will give mode shape with amplitude in the unit of the FRF. Here $m/s^2/N$, which amplify the amplitude of the higher modes for acceleration modes. We can note the regular mesh created by the triangulation from the irregular measurement positions (red stars).

7.3 Short Analysis of the method accuracy on mode shapes examples

In the following figures are illustrated the main bending modes shapes of the deck along the X direction.

It is important to note that the modes are very well identified from the different shapes as it is shown in the Figure 18, and Figure 19 as examples.

The frequencies have a rather narrow dispersion with respect the different output transducers. The dispersion increase when the mode coupling is important which is the case of the first bending mode.

The values of damping are overestimated due to the identification methodology and because most of the modes are strongly coupled to torsion or “flapper” modes.

From the analysis of the Figure 18 and Figure 20 we can highlight how the FIHT is accurate, as the measurements show perfectly the exact boundary condition. In that case, a rigid support will have shown no displacement at the support; here we can observe that the support are elastic, (made of rubber from the designer).

This is a very important result for the method, as it can bring to the model designer, information of high interest on the boundary conditions, which are most often affected of important error in the numerical analysis.

When different types of transducers are used on the same structure, some correlation checks are also possible to reinforce the quality of the measurements. It is the case here, between the displacement and the acceleration transducer for the first bending mode, which are phased of 180 degrees each other. Another remark from the mode shape display of the Figure 18, is, how the mode shape amplitude is dependant of the transducer type; for low modes, we have large displacement amplitude and much smaller for acceleration amplitude caused by the ratio of the square of the frequency.

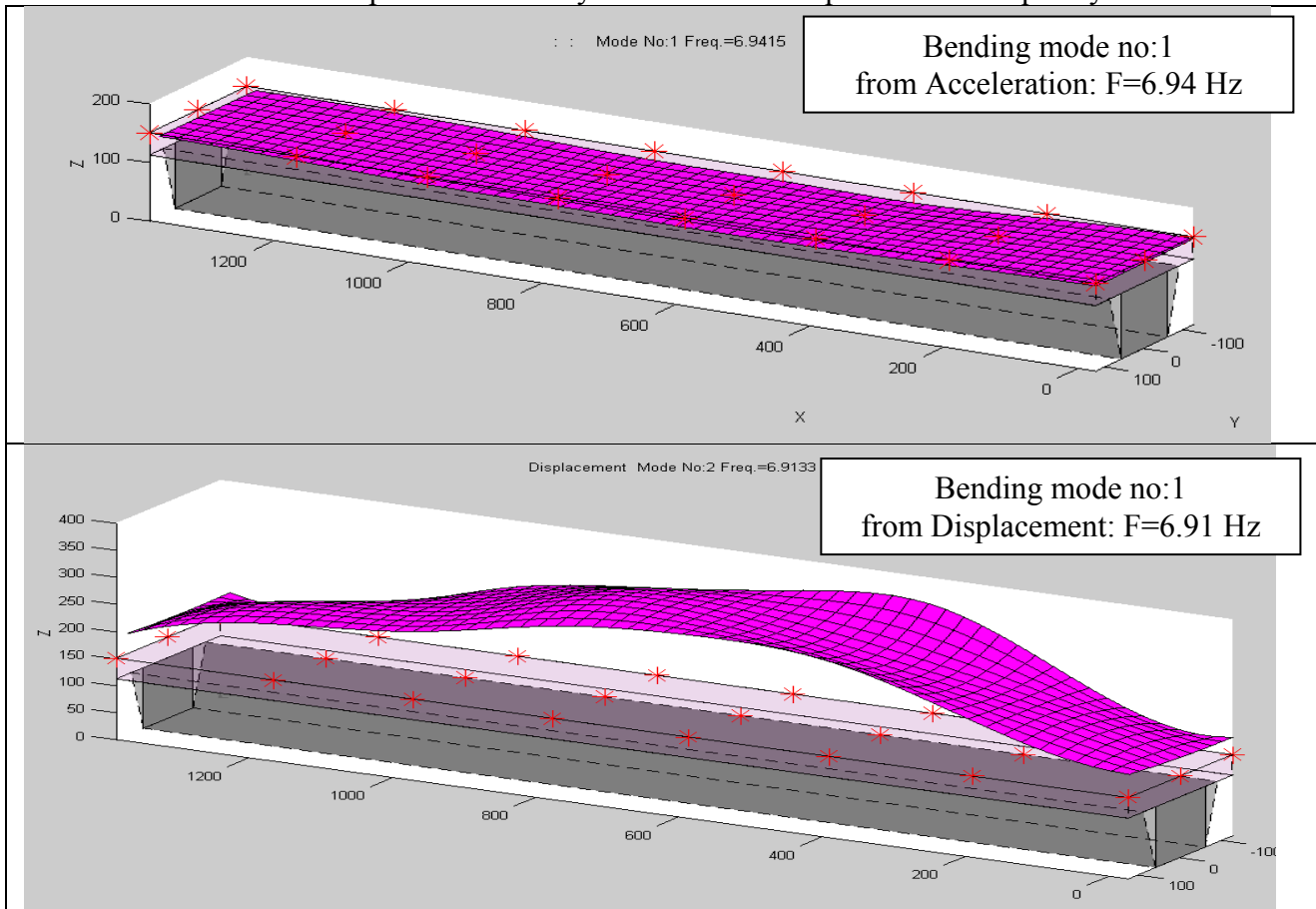


Figure 18: example of mode shapes of the same bending mode (no: 1) measured from acceleration above, and from displacement below.

Finally the accuracy of the method is here still well illustrated by the regularity of the acceleration mode shape with respect the displacement mode shape which is affected by an important noise in the signals, giving irregularity in the shape.

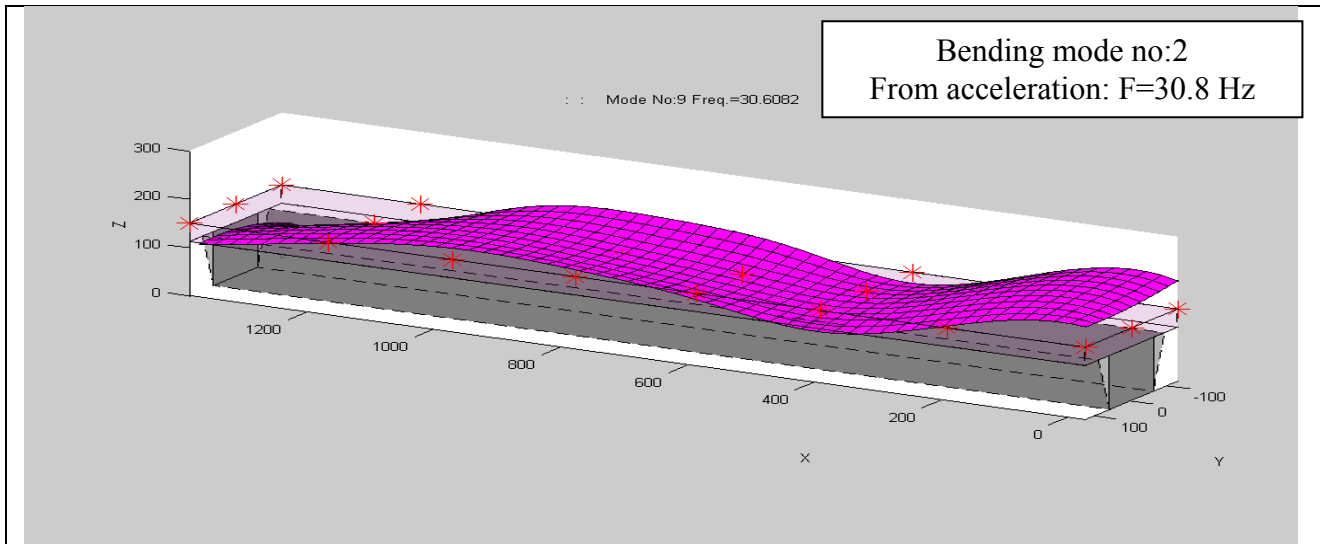


Figure 19: mode shape of the second bending mode (In “free free” condition) measured in acceleration

It is important to note in the Figure 19, that the bending mode measured is a typical bending no: 2 for a beam in free-free edges. The mode (as all bending modes) is obtained with a good accuracy due to the important number of points measured. From that it could be possible to quantify the elasticity of the supports as the deflection of the deck is very important at the level of the rubber support abscissa. Another kind of mode also identified by the method, which is a non structural mode, where the deck in that case has no strain (in the error limit of the measurements). It is a rotation of the deck on its centre, due to the elasticity of the support.

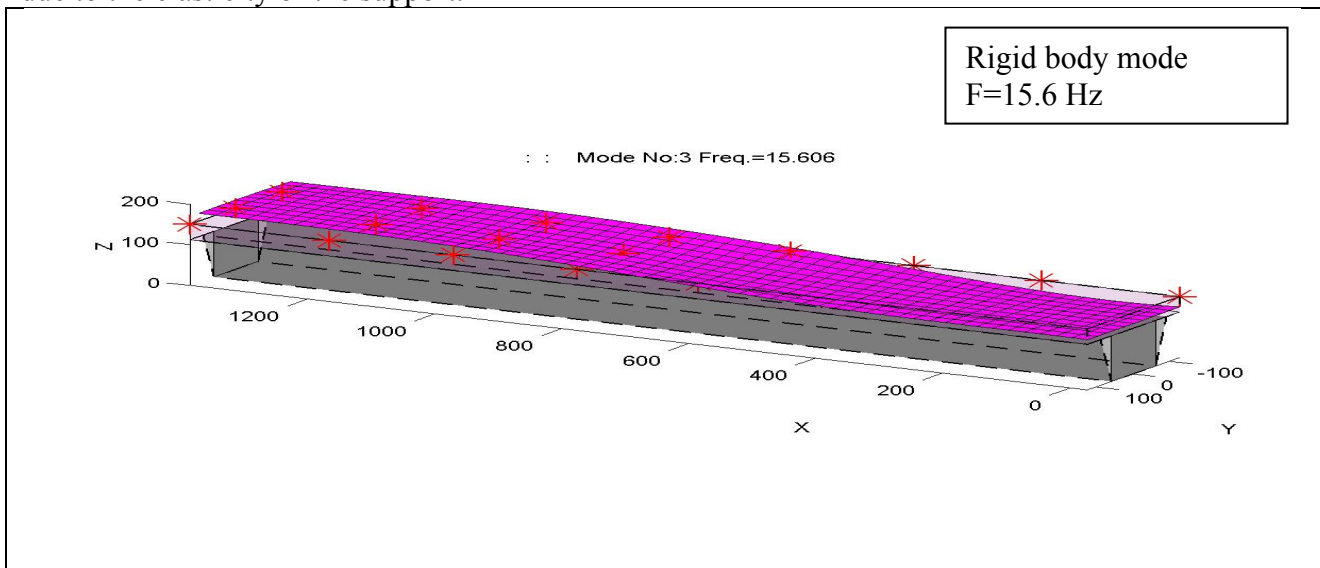


Figure 20: Rigid body mode shape of the deck on the elastic supports

This measurement bring also information on the boundary conditions, which seems to be closer to “free-free” beam than a “simply supported “ beam as expected.

Finally we can illustrate two important remarks on the method, by the comparison of the modes shapes of the Figure 19 and the design of the mode shape of the Figure 21.

First, even the frequency difference between the modes is small (30.8 for the bending and 29.5 for the torsion) the shapes are completely different which means that the instrument, but mainly the method extraction and peak-grouping is sufficiently efficient to separate the two kinds of dynamic behaviours.

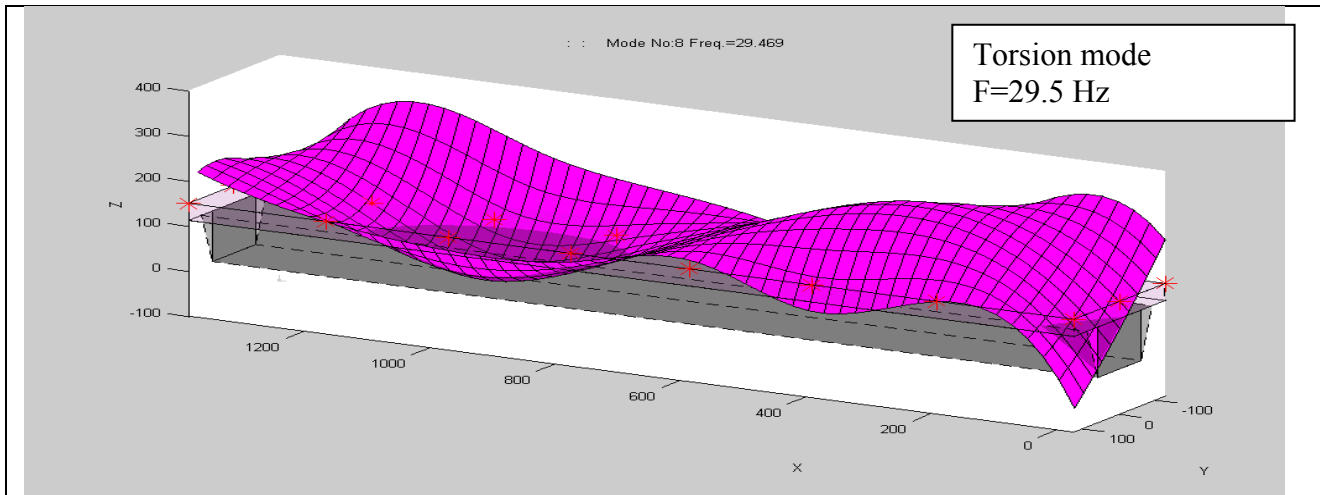


Figure 21: Main torsion mode coupled to a flapper mode of the deck. From acceleration measurements

The second remark concerns the amplitude of the modes. It is clear from the Figure 21 and Figure 18 that torsion amplitude is much higher than bending, and this could be seen on the FRF curves. It is confirmed by the geometry of the bridge which is stiffer in X direction and more flexible on each side of the deck width. The method is still here enough efficient, to compare the level of flexibility for each type of modes.

8 Implementation of the Logarithmic Decrement in the FIHT Method for Accurate Damping Measurement

As the half power band method used in FIHT is not very accurate for the evaluation of the damping in the structure, as is shown on the Figure 22, for each of the mode extracted, the toolbox of the FIHT contains a special function adapted to the evaluation of the damping from time signals.

With this option, and only if a doubt exists on the results obtained with the FIHT method, as is the case above, the damping value could be extracted from time signal after an automatic digital filtering as shown on the Figure 23. In the example (first bending mode at 6.9 Hz) the problem of damping error due to the method seems solved by the application of the function.

It is important to mention that in the case of modes highly coupled it is very difficult to get an automatic filter able to reject one of them. This inconvenient is one of the main limitations of the automation process of the function here described. Parameters extraction in particular cases as the one mentioned before always causes problems of identification with nearly all the methods.

It is more convenient, if necessary, to perform other tests, addressed to the specific case to remove the uncertainty. If a fast processing is possible as it is the case with the FIHT, the knowledge of the problem will be discovered in time before the instrumentation is removed, and others tests are possible.

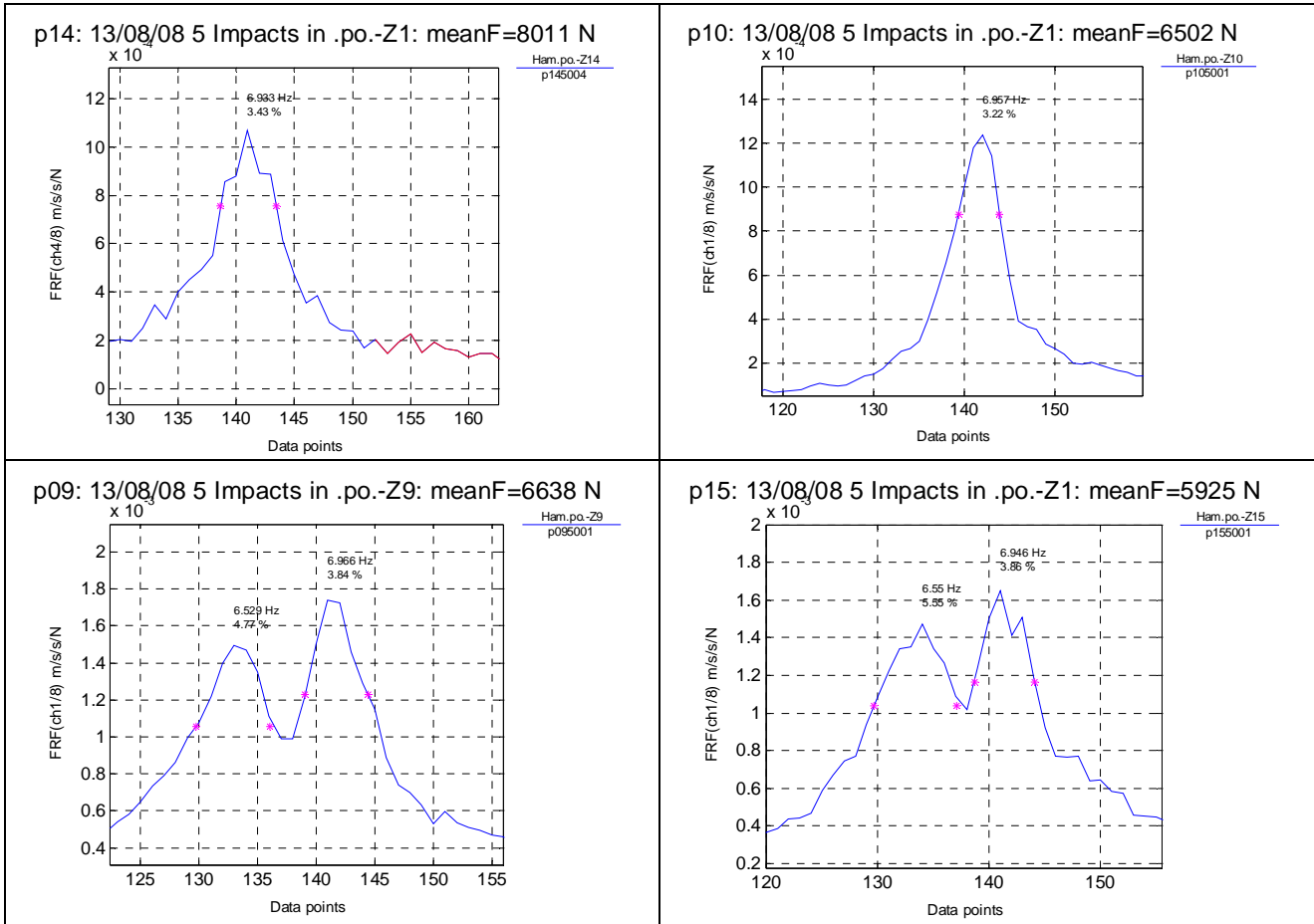


Figure 22: Case of high coupling between modes (bending 1 and flapper modes) giving not accurate damping values

Concerning the practical aspect of the use of the function, the automation required only the mode number you want to apply the procedure, then the routine displays the filtered signal with the damping found and the error between the experimental envelopes (irregular in that case) and the fitted equation. The damping is calculated by fitting the mean of the two experimental envelopes, (envelop of maxima and envelop of minima) with a decreasing exponential function, which the parameters give the equivalent viscous damping of the signal. The fitting is performed under Matlab using the simplex optimisation method.

An example is shown below, which correspond to the upper right extraction (p10) of the Figure 22.

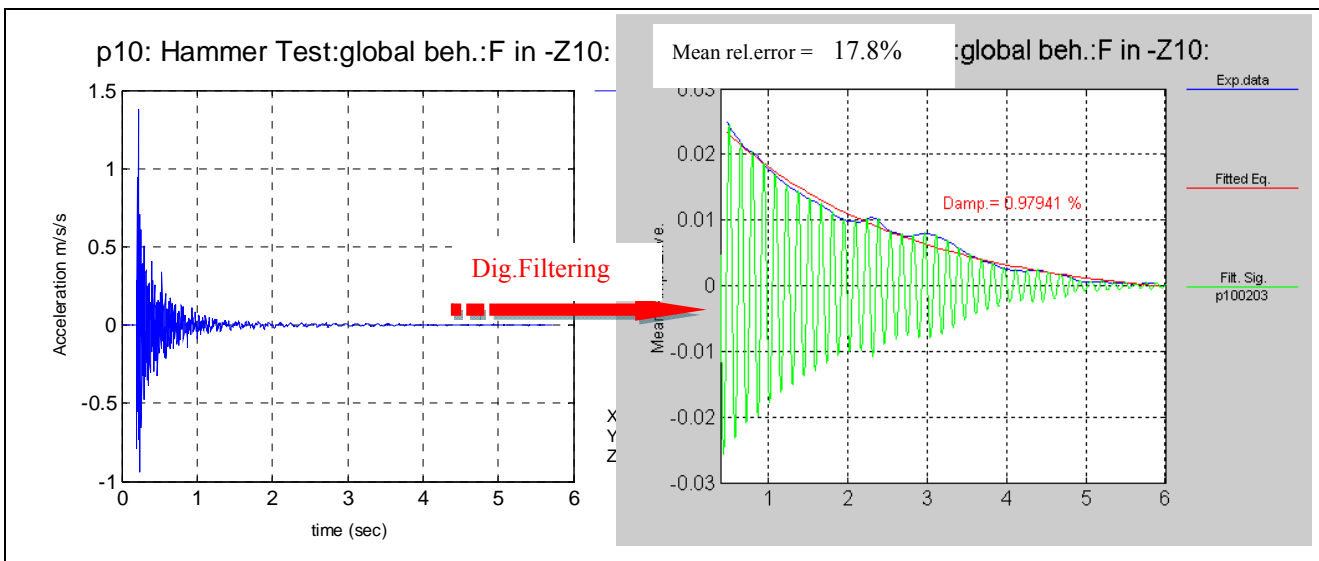


Figure 23: global damping evaluation by the envelopes decay fitting, on a filtered signal of acceleration.

9 Conclusion

The Fast Impact Hammer Testing method implemented and described in the example above and used for modal testing, have proved to be very efficient in time saving, both for the tests and for the signal processing, and without reducing the accuracy. The method has been used with success, also on real structures, as the Spanish motorway bridge shown in example, and on the real scale frames tested in the ELSA laboratory.

Since the procedure is totally experimental, founded mainly on statistical treatments, one can complain on the absence of a model. However the aim is to perform experimental modal analysis in situ so to have quickly the main results, to be sure that the measurements are accurate and their space distribution is appropriate. The method helps also to decide if others measurements are needed, cancelling the doubt that the tests number is insufficient.

Engineers performing experimental analysis know very well the unexpected dynamic behavior of a real structure with respect to numerical models and it is fundamental to have a tool which can bring a quick response to confirm or not model results. The FIHT method, for small and medium structures is part of these objectives; moreover it enables to highlight the presence of difficulties in extracting modes, and therefore guides the engineer to choose another method (commercial powerful tool) more apt to solve the problem encountered.

The main achievements in the FIHT method are:

For the tests, the use of the reciprocity of the transfer functions.

For the processing, it is the use of coherence histogram coupled with the FRF filtering and mapping, which introduce a novelty in the field. Finally the modal procedure extraction is drastically reduced and eased by the use of criteria and statistic treatment based on a large campaign of experimental modal analysis.

It is important to note that, even the time needed is shorter than in traditional methods, the accuracy is generally globally increased as the points measured in the structure could be generally much more than in traditional modal testing where the number of accelerometers is limited. This last remark shows that the FIHT method is able to give an improvement to the experimental methods used in non destructive testing of civil structures.

However the method needs to be improved for a “real-time” use, which is part of one task of the SERIES project.

References

- [1] *Daniel Tirelli, Stefano Primi, Eugenio Gutiérrez*. Experimental Modal Analysis of PUMACOM Carbon-Fibre Composite Highway Bridge at Crossing PK 1+640 of the Autovía del Cantábrico. Dynamic load test. Report No:1 .2004. European Laboratory for Structural Assessment, IPSC, Joint Research Centre. Commission of the European Communities, Ispra, Italy.
- [2] *Armelle Anthoine and Daniel Tirelli*. Project No. Coll – Ct - 2003 – 500291. ESECMaSE. Enhanced Safety and Efficient Construction of Masonry Structures in Europe. Work Package N° 8. D 8.2 Preliminary tests and dynamic identification of the specimens. 04/07/2008. Draft N°1. European Laboratory for Structural Assessment (ELSA) . Joint Research Centre of the European Commission .21020 Ispra (VA). Italy .
- [3] *N. M.M. Maia, J. M.M. Silva*, Instituto Superior Tecnico, Portugal. Theoretical and Experimental Modal Analysis, RSP, Research Studies Press LTD. Taunton Somerset England.
- [4] *D.J. Ewins*, Professor of Vibration Engineering, Imperial College of Science and Technology, London, England.RSP Research Studies Press LTD. Letchworth, Hertfordshire, England- Bruel & Kjaer.
- [5] *DynaWorks*, un produit Intespace. The CATSMoDal/STAR6 System™ BP4356 31029 Toulouse cedex 4, France. Web:<http://www.dynawork.com>.
- [6] *Etienne Balmes*, Orthogonal Maximum Sequence Sensor Placements Algorithms for modal tests, expansion and visibility. SDTools and Ecole Centrale.Paris/MSSMat, balmes@sdtools.com
- [7] *ARTEMIS Extractor Artemis*. Structural Vibration Solutions A/S • Tel: +45 9635 4422 • Fax: +45 9635 4575 • svibs@svibs.com
- [8] *ME'scope VES 4.0*, Visual Engineering series Vibrant Technology, Inc. 5 Erba Lane, Suite BScotts Valley, CA 95066. WWW:<http://www.vibetech.com>
- [9] *O.S.Bursi, J.Molina, W.Salvatore, and F. Taucer*. Dynamic Characterisation of a 3D full scale steel concrete composite building at ELSA. EUR21206 EN.
- [10] *M. Poljanšek, G. Bof, P. Capéran, J. Esteves, E. Gutiérrez, O. Hubert, R. Kiefer, D. Tirelli, B. Viaccoz, A. Zorzan*. Report on Testing and Analysis of PROMETEO Fibre Reinforced Composite Bridge Beam. Limited Distribution PUBSY JRC54320 – 2009.
- [11] *F. J. Molina, R. Pascual and J.-C. Golinval*, DESCRIPTION OF THE STEELQUAKE BENCHMARK, Mechanical Systems and Signal Processing (2003) 17(1), 77–82.
- [12] *Christoph Heinemeyer, Christiane Butz, Andreas Keil, Mike Schlaich, Arndt Goldack, Stefan Trometer, Mladen Lukić, Bruno Chabrolin, Arnaud Lemaire, Pierre-Olivier Martin, Álvaro Cunha, Elsa Caetano*. Design of Lightweight Footbridges for Human Induced Vibrations Background document in support to the implementation, harmonization and further development of the Eurocodes. Editors: G. Sedlacek, Chr. Heinemeyer, Chr. Butz together with M. Géradin JRC First Edition, May 2009 EUR 23984 EN.

- [13] *C. Rainieri and G. Fabbrocino*, Automated output-only dynamic identification of civil engineering structures, *Mechanical Systems and Signal*, Mechanical Systems and Signal processing, Volume 24, Issue 3, Pages 678-695.
- [14] *Dimitry N. Zotkin, a_ Ramani Duraiswami, b_ Elena Grassi, c_ and Nail A. Gumerov*, Perceptual Interfaces and Reality Laboratory, Institute for Advanced Computer Studies (UMIACS), University of Maryland at College Park, College Park, MD 20742 Fast head-related transfer function measurement via reciprocity May 2006.
- [15] *Scott w. Doebling and Charles r. Farrar*. Engineering Analysis Group (ESA-EA), Los Alamos National Laboratory, Los Alamos, NM, 87545, USA. Estimation Of Statistical Distributions For Modal Parameter From Averaged Frequency Response Function Data. *Journal of Vibration and Control*, July 2000
- [16] *Michele Frizzarin¹, Maria Q. Feng², Paolo Franchetti¹, Serdar Soyoz². and Claudio Modena*
¹= Department of Structural and Transportation Engineering, University of Padova, Italy
²=Department of Civil and Environmental Engineering, University of California, Irvine, U.S.A.
 Damage detection based on damping analysis of ambient vibration data. *Struct. Control Health Monit.* (2008)
- [17] *Jean Piranda*. Professeur à l'Université de Franche Comté. Laboratoire de Mécanique Appliquée R. Chaleat. Analyse modale expérimentale. Section De cooperation Doc 2008.à
- [18] *A. Pavic R. Pimentel and P. Waldron*. University of Sheffield. Centre for Cement and Concrete. Department of Civil and Structural Engineering. Sheffield S1 3JD. UK.
 Instrumented Sledge Hammer Impact Excitation: worked examples.
- [19] *A.M. Fareed, G Schmidt, F. Wahl*. Experimental Identification of Modal density Parameters of Light Weight Structures. *Technische Mechanik*, Band 21 Heft 3 (2001) 215-225.
- [20] *Ernst Forstner*. Experimentelle Untersuchung des Schwingungsverhaltens externer Spannglieder . Diplomingenieur für Kulturtechnik und Wasserwirtschaft an der Universität für Bodenkultur Wien. November 2003.

Annex 1

Examples of “beam” and “irbeam” matlab functions used in the FIHT toolbox to help to a quick built of simples structures or deformed structures

The first utility of these 2 functions is, when in the group of FRFs of the structure tested, if the corner (or extremity) positions are all part of the experiments, then an automatic generation of the structure could be performed using only the coordinate of the FRFs position, already inserted before the signal processing. In other cases the extremities could be inserted as “virtual” transducers.

Help of the Function “beam”

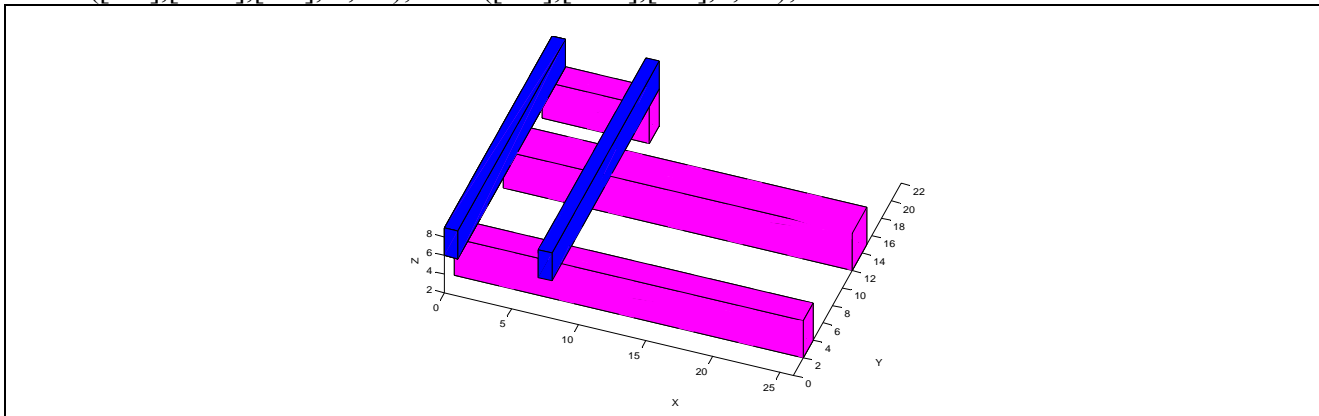
```
function [Sx,Sy,Sz] = beam(x,y,z,nf,color)
%[Sx,Sy,Sz] = beam(x,y,z,nf)
%Beam Generation with rectangular section. The vectors x,y,z must be in the same
unit.
% generate a beam on 3 axes with the following dimensions and positions:
% dimensions are equal to the maximum and minimum of each vectors x,y,z.
% DEFAULT: if one of the vector x,y or z is empty its default values are:
% [0 (beam length)/20], where length is the maximum length of the 3 directions.
% The position of the beam plotted in the 3D figure, starts at the minima of
% x, y, and z. Default is 0.
% nf= figure number where the beam is plotted(default=new figure).
% color= color of the face of the beam.
% Sx,Sy,Sz are the 3 components(matrix) of the mesh to be plotted.

%Examples:
%      beam([0 1 2 4 8 18 26],[],[2 4 6],10,'magenta');
%plot a beam on the figure 10, of length of 26 and with a section of (26/20)X4
and cantered to 4 in z direction, and 1.3 (=26/20*2) in Y direction.
%      beam(coor(:,1),coor(:,2),coor(:,3));
%plot in the existent figure with the default color (black), a beam which %include
all the points defined in the coordinate matrix coor.

% See functions IRSBEAM (for beam with irregular sections)
%      PLACETRANS (for transducers positions design)
%      INPUTCARTE (for inputs mapping)
%      COHERCARTE ( for coherence mapping)
```

An example of a series of beam function used for a structural design give the following results in the figure below. Note that for the 1st coordinate of the first beam, inserting [0 26] will gives the same result.

```
beam([0 1 2 4 8 18 26],[12 15],[2 6],3,'magenta');
beam([0 1 2 4 8 18 26],[12 15],[2 6],3,'magenta');
beam([0 1 2 4 8],[20 22],[2 6],3,'magenta');
beam([0 1],[0 22],[6 9], 3,'b');beam([7 8],[0 22],[6 9],3,'b');
```



Help of the function "irsbeam"

```
function [Sx,Sy,Sz] = irsbeam(x,y,z,nf,color)
%[Sx,Sy,Sz] = irsbeam(x,y,z,nf,color)
%Beam Generation with irregular section. The vectors x,y,z must be in the same
unit.
% generate a beam on 3 axes with the following dimensions and sections:
% one of the vector (axes) must have 2 numbers which represent the two extrem
positions of the beam.
% the two others vectors must have the same number of points sufficient to
describe the irregularity
% of the irregular section. If the section is in the plane (x,y) x0=xfinal, and
yo=yfinal.
% DEFAULT:if one of the vector x,y or z is empty its default values are:[0 (beam
length)/20]
% nf= figure number where the beam is plotted(default=new figure).
% color= color of the face of the beam.
% Sx,Sy,Sz are the 3 components(matrix) of the mesh to be plotted.
%
%Example: irsbeam([-28 1385],[60 -60 -90 90 60],[0 0 112 112 0],10,'magenta');
%plot a beam on the figure 10, of length in x direction between position -28 to
1385 with an irregular section in y and z direction describes by 5 points of
coordinates y(1:5)and z(1:5).
%
%See functions BEAM (for beam with regular sections).PLACETRANS (for tansducers
positions design).
```

An example of 3 irregular beams (irsbeam) is shown on the figure below associated with the cylinder function used for the pears of the bridge designed.

- Plot of the Deck and of the carbon beam in grey:

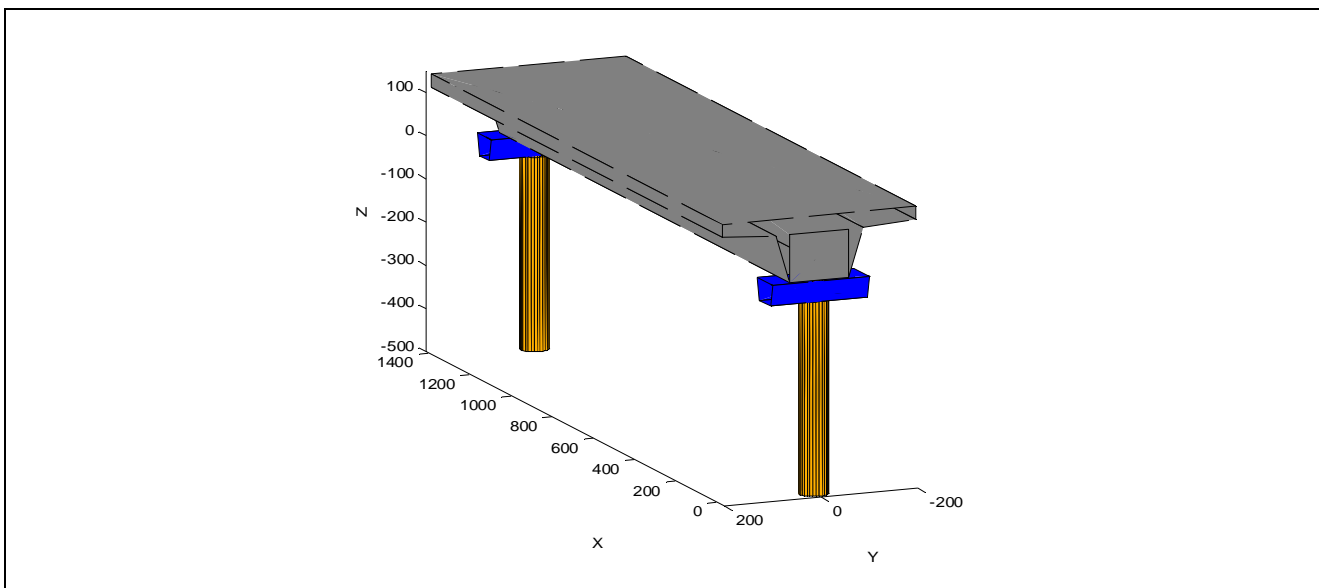
```
irsbeam([-28 1385],[60 -60 -90 -200 -200 200 200 90 60],[0 0 112 120 150 150 120 112 0],[,],[.5 .5
.5]);
```

- Left and right supports of the deck in blue:

```
irsbeam([-28 -38 38 28 -28],[-100 100],[-50 0 0 -50 -50],3,'b'); irsbeam([1339 1329 1395 1385
1339],[-100 100],[-50 0 0 -50 -50],3,'b'); hold on;
```

- Left and right cylindrical pears:

```
[x1,y1,z1]=cylinder(28,30); z1=z1*(-450);
z1=z1-50;surf(x1,y1,z1);x2=x1+1357 ;y2=y1 ;z2=z1 ;surf(x2,y2,z2);
```



European Commission

EUR 24964 EN– Joint Research Centre – Institute for the Protection and Security of the Citizen

Title: Modal Analysis of Small & Medium Structures by Fast Impact Hammer Testing Method

Author: Daniel Tirelli

Luxembourg: Publications Office of the European Union

201 – 39 pp. – 21,0 x 29,7 cm

EUR – Scientific and Technical Research series – ISSN 1831-9424

ISBN 978-92-79-21479-0

doi: 10.2788/80576

Abstract

In the context of the SERIES project (Task 2.3: “*software development for data processing*”) concerning the availability of simple tools and techniques for real-time data analysis and interpretation, the present report discusses the use of the Fast Impact Hammer Testing method (FIHT) with the purpose of providing to the partners of SERIES the opportunity to use the FIHT method on the structures of the project, and at the same time to improve the method for the dynamic characterisation of structures. The method is illustrated using a practical example of a novel type of structure tested at ELSA, named PROMETEO, composed of a concrete and fibre glass deck supported by a carbon fibre beam 13 meters long. The results obtained with the FIHT method was compared with the results obtained by others existing methods and on other types of structures, confirming the validity of the new methodology employed. The ease of use, and the reduced test and processing time, are the main advantages and improvements with respect to traditional and formal methods used in civil engineering.

How to obtain EU publications

Our priced publications are available from EU Bookshop (<http://bookshop.europa.eu>), where you can place an order with the sales agent of your choice.

The Publications Office has a worldwide network of sales agents. You can obtain their contact details by sending a fax to (352) 29 29-42758.

The mission of the JRC is to provide customer-driven scientific and technical support for the conception, development, implementation and monitoring of EU policies. As a service of the European Commission, the JRC functions as a reference centre of science and technology for the Union. Close to the policy-making process, it serves the common interest of the Member States, while being independent of special interests, whether private or national.

